Interplay between aggregation number, micelle charge and hydration of catanionic surfactants

Supplementary Information

Žiga Medoš[1]

Sergej Friesen[2]

Richard Buchner[2]*

Marija Bešter-Rogač[1]*

[1]Faculty of Chemistry and Chemical Technology, Večna pot 113, University of Ljubljana, SI-1000 Ljubljana, Slovenia

[2]Institut für Physikalische und Theoretische Chemie, Universität Regensburg, 93053 Regensburg, Germany

*Corresponding authors:

Prof. Dr. Marija Bešter-Rogač

Faculty of Chemistry and Chemical Technology, Večna pot 113, 1000 Ljubljana, Slovenia

E-mail address: marija.bester@fkkt.uni-lj.si

Prof. Dr. Richard Buchner

Institut für Physikalische und Theoretische Chemie, Universität Regensburg, 93053 Regensburg, Germany

E-mail address: Richard.Buchner@chemie.uni-regensburg.de

Table of Contents

Example of raw signal during isothermal titration calorimetry

Figure S1. Raw signal (heat flow, q) as a function of time, t, with subtracted baseline as obtained from the VP-ITC microcalorimeter for $[C_{10}Me_3N]^+[C_8]^-$ at 298.15 K. Each peak corresponds to the heat effect at the addition of 3 µL surfactant solution.

Densities of investigated systems

Experimental values of densities of water solutions for all studied systems in the temperature range between 278.15 and 328.15 K are presented in Figure S1 and Table S1.

Table S1. Concentrations, m, and densities, ρ, of prepared solutions of studied systems between 278.15 and 328.15 K.

m/ mol·kg^{-1} solution	ρ/kg·dm^{-3}					
	278.15 K	288.15 K	298.15 K	308.15 K	318.15 K	328.15 K
$[C_6Me_3N]^+[C_{10}]^-$						
0.029970			0.996548			
0.075187			0.995444			
0.099260			0.994812			
0.147274			0.993558			
0.199098			0.992201			
0.249580			0.990884			
0.445961	0.991456	0.989068	0.985834	0.981893	0.977340	0.972249
0.521610			0.984706			
1.073622			0.971420			
$[C_8Me_3N]^+[C_{10}]^-$						
0.015037			0.996732			
0.030628	0.999471	0.998435	0.996258	0.993154	0.989267	0.984693
0.076751	0.998297	0.997098	0.994795	0.991590	0.987621	0.982980
0.099199			0.994094			
0.150020			0.992476			
0.198922			0.991123			
0.200449			0.990870			
0.209017	0.994907	0.993269	0.990614	0.987128	0.982936	0.978121
0.248579			0.988996			
0.496429			0.982120			
0.589536			0.979202			
$[C_8Me_3N]^+[C_8]^-$						
0.029985			0.996558			
0.05001			0.996253			
0.059992			0.996068			
0.075474			0.995620			
0.098044			0.995031			
0.149920			0.993662			
0.199810			0.992329			
0.249286			0.991032			
0.552238	0.989435	0.986628	0.983075	0.978885	0.974136	0.968884
0.681490			0.98060			
1.072229			0.97060			

Table S1. continued

m/ mol·kg^{-1} solution	ρ/kg·dm^{-3}					
	278.15 K	288.15 K	298.15 K	308.15 K	318.15 K	328.15 K
$[C_{10}Me_3N]^+[C_{10}]^-$						
0.001025	0.999959	0.999082	0.997020	0.994003	0.990183	0.985661
0.002016	0.999940	0.999062	0.997003	0.993982	0.990155	0.985629
0.003039	0.999930	0.999046	0.996978	0.993960	0.990131	0.985602
0.005059	0.999900	0.999006	0.996931	0.993899	0.990064	0.985533
0.010112	0.999778	0.998850	0.996751	0.993706	0.989864	0.985324
0.015176	0.999638	0.998690	0.996580	0.993522	0.989667	0.985120
0.020265	0.999491	0.998523	0.996397	0.993327	0.989462	0.984908
0.030324	0.999231	0.998215	0.996053	0.992952	0.989065	0.984493
0.040197	0.998876	0.997823	0.995628	0.992507	0.988603	0.984019
0.050189			0.995259			
0.073087	0.997875	0.996704	0.994418	0.991216	0.987248	0.982614
0.080077			0.994291			
0.097971			0.993296			
0.104362	0.996848	0.995580	0.993250	0.989998	0.985969	0.981288
0.119851			0.992880			
0.120727	0.996368	0.995097	0.992700	0.989389	0.985332	0.980624
0.124281	0.996230	0.994955	0.992535	0.989243	0.985180	0.980471
0.150377			0.991512			
0.188838			0.990485			
0.200935			0.989638			
0.249329			0.987844			
0.295139	0.990888	0.989064	0.986253	0.982573	0.978205	0.973251
$[C_{10}Me_3N]^+[C_8]^-$						
0.030382	0.999488	0.998446	0.996264	0.993159	0.989269	0.984694
0.075919	0.998322	0.997118	0.994812	0.991607	0.987639	0.983000
0.101085			0.994094			
0.149685			0.992473			
0.199758			0.990860			
0.207720	0.994890	0.993247	0.990591	0.987107	0.982916	0.978102
0.249732			0.989264			
$[C_{10}Me_3N]^+[C_6]^-$						
0.029174	0.999665	0.998687	0.996540	0.993450	0.989562	0.984981
0.073437	0.999118	0.997855	0.995515	0.992291	0.988307	0.983658
0.097474	0.998626	0.997275	0.994872	0.991598	0.987576	0.982896
0.133544	0.997882	0.996414	0.993920	0.990571	0.986489	0.981763
0.195111	0.996580	0.994915	0.992263	0.988791	0.984612	0.979805
0.243846	0.995593	0.993778	0.991006	0.987436	0.983181	0.978318
0.440527	0.991474	0.989047	0.985788	0.981831	0.977267	0.972160
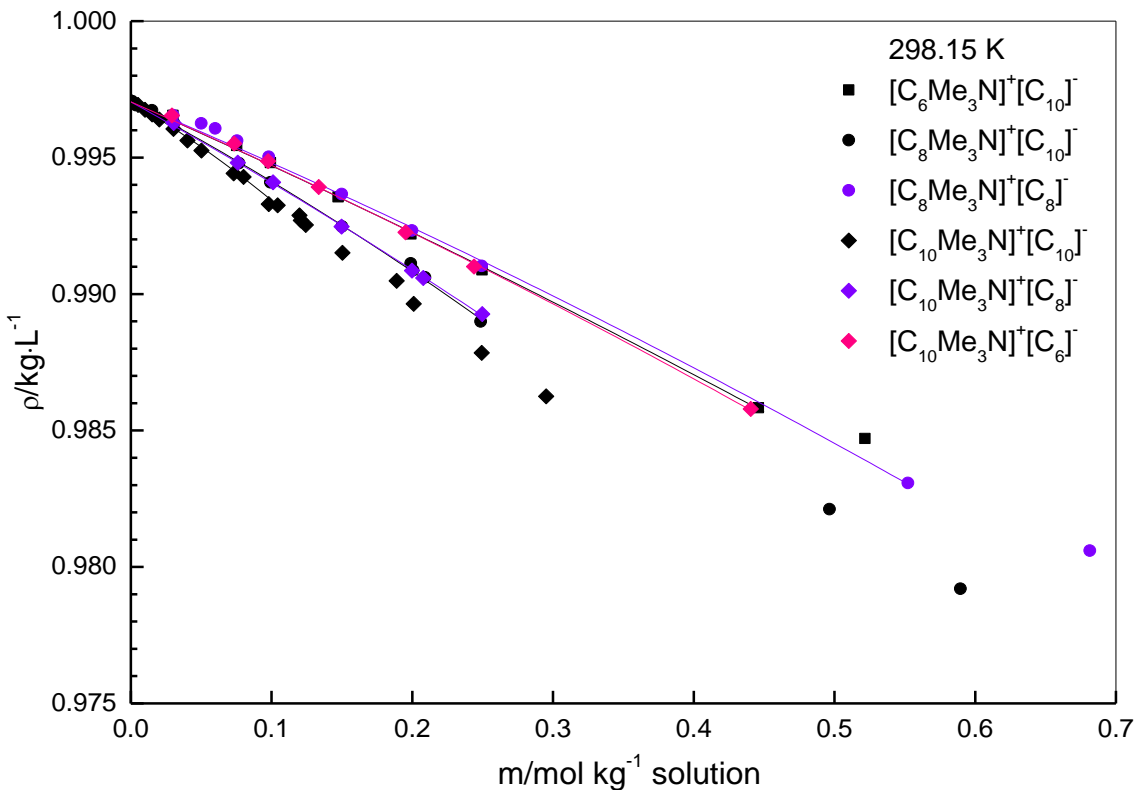
Figure S2. Densities of water solutions for $[C_xMe_3N]^+[C_y]^-$ at 298.15 K. Lines represents the polynomial fits by eq. (i) using coefficients from Table S2.

In the specified concentration range the measured densities of studied systems were fitted to eq i,

$$\rho(T,m) = a(T)m^2 + b(T)m + \rho_{H_2O}(T) \tag{i}$$

where m is the concentration in mol of surfactant per kg of the solution. The coefficients $a(T)$ and $b(T)$ for all investigated systems at all temperatures are given in Table S2 and Figure S2 together with the literature data for density of water, ρ_{H_2O}.[1]

For ITC experiments eq i was used to calculate the densities of solution in the titration cell after each addition of stock solution.

Table S2. Densities of water[1] and coefficients a and b in eq i for $[C_xMe_3N]^+[C_y]^-$ used to convert concentration scale in the range between 0 *and* m_{max}.

$T/$ K	$\rho_{H_2O}/$ kg·dm^{-3}		$m_{max}/$ mol·kg^{-1}	$a/$ kg^3·mol^{-2}·dm^{-3}	$b/$ kg^2·mol^{-1}·dm^{-3}
278.15	0.999964	$[C_8Me_3N]^+[C_{10}]^-$	0.21	-0.02490	-0.01902
		$[C_{10}Me_3N]^+[C_{10}]^-$	0.10	-0.08830	-0.02066
		$[C_{10}Me_3N]^+[C_8]^-$	0.20	-0.02777	-0.01869
		$[C_{10}Me_3N]^+[C_6]^-$	0.44	-0.01154	-0.01434
288.15	0.999101	$[C_8Me_3N]^+[C_{10}]^-$	0.21	-0.01849	-0.02406
		$[C_{10}Me_3N]^+[C_{10}]^-$	0.10	-0.07109	-0.02633
		$[C_{10}Me_3N]^+[C_8]^-$	0.20	-0.02068	-0.02391
		$[C_{10}Me_3N]^+[C_6]^-$	0.44	-0.00859	-0.01916
298.15	0.997043	$[C_6Me_3N]^+[C_{10}]^-$	0.45	-0.00528	-0.02288
		$[C_8Me_3N]^+[C_{10}]^-$	0.25	-0.01887	-0.02732
		$[C_8Me_3N]^+[C_8]^-$	0.55	-0.00657	-0.02174
		$[C_{10}Me_3N]^+[C_{10}]^-$	0.10	-0.06094	-0.03000
		$[C_{10}Me_3N]^+[C_8]^-$	0.25	-0.01152	-0.02849
		$[C_{10}Me_3N]^+[C_6]^-$	0.44	-0.00691	-0.02261
308.15	0.994036	$[C_8Me_3N]^+[C_{10}]^-$	0.21	-0.01239	-0.03048
		$[C_{10}Me_3N]^+[C_{10}]^-$	0.10	-0.04286	-0.03436
		$[C_{10}Me_3N]^+[C_8]^-$	0.20	-0.01382	-0.03050
		$[C_{10}Me_3N]^+[C_6]^-$	0.44	-0.00566	-0.02530
318.15	0.99022	$[C_8Me_3N]^+[C_{10}]^-$	0.21	-0.01058	-0.03265
		$[C_{10}Me_3N]^+[C_{10}]^-$	0.10	-0.04518	-0.03602
		$[C_{10}Me_3N]^+[C_8]^-$	0.20	-0.01185	-0.03272
		$[C_{10}Me_3N]^+[C_6]^-$	0.44	-0.00476	-0.02738
328.15	0.98570	$[C_8Me_3N]^+[C_{10}]^-$	0.21	-0.00916	-0.03436
		$[C_{10}Me_3N]^+[C_{10}]^-$	0.10	-0.04277	-0.03782
		$[C_{10}Me_3N]^+[C_8]^-$	0.20	-0.01044	-0.03442
		$[C_{10}Me_3N]^+[C_6]^-$	0.44	-0.00407	-0.02901

Figure S3. Coefficients *a* and *b* in eq i of $[C_xMe_3N]^+[C_y]^-$ in the concentration range of the solution as presented in Table S2.

Figure S4. Concentration dependence of the apparent molar volumes, V_ϕ, of aqueous solutions for $[C_xMe_3N]^+[C_y]^-$ at 298.15 K.
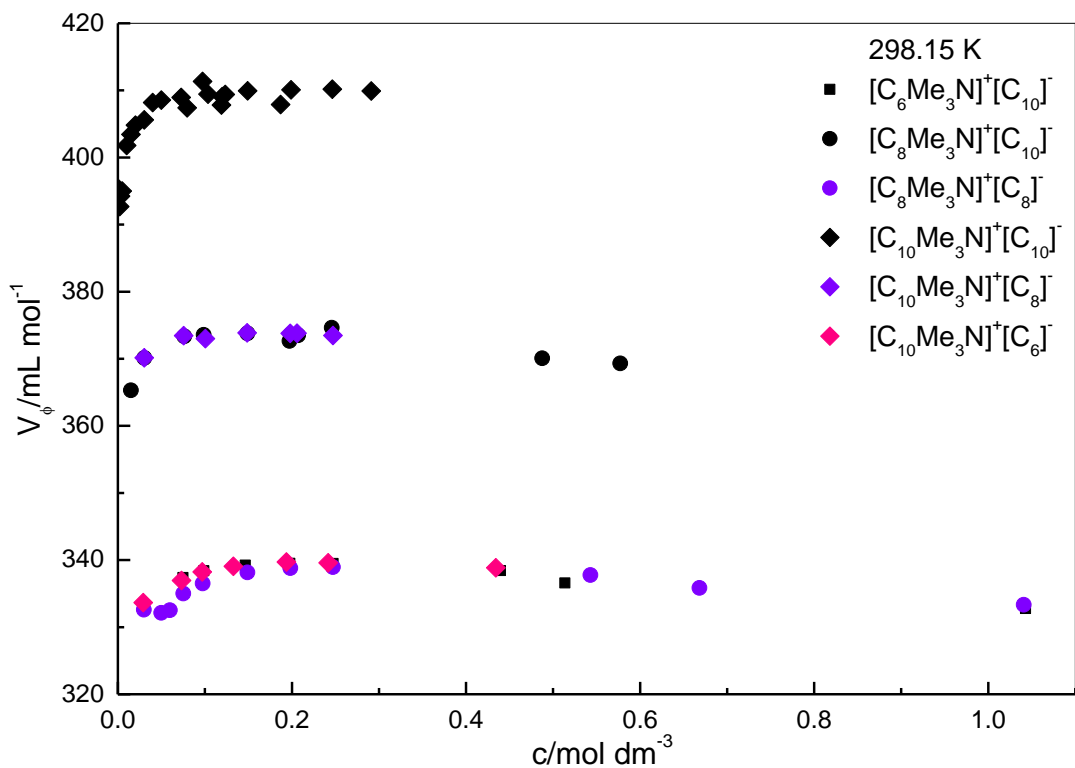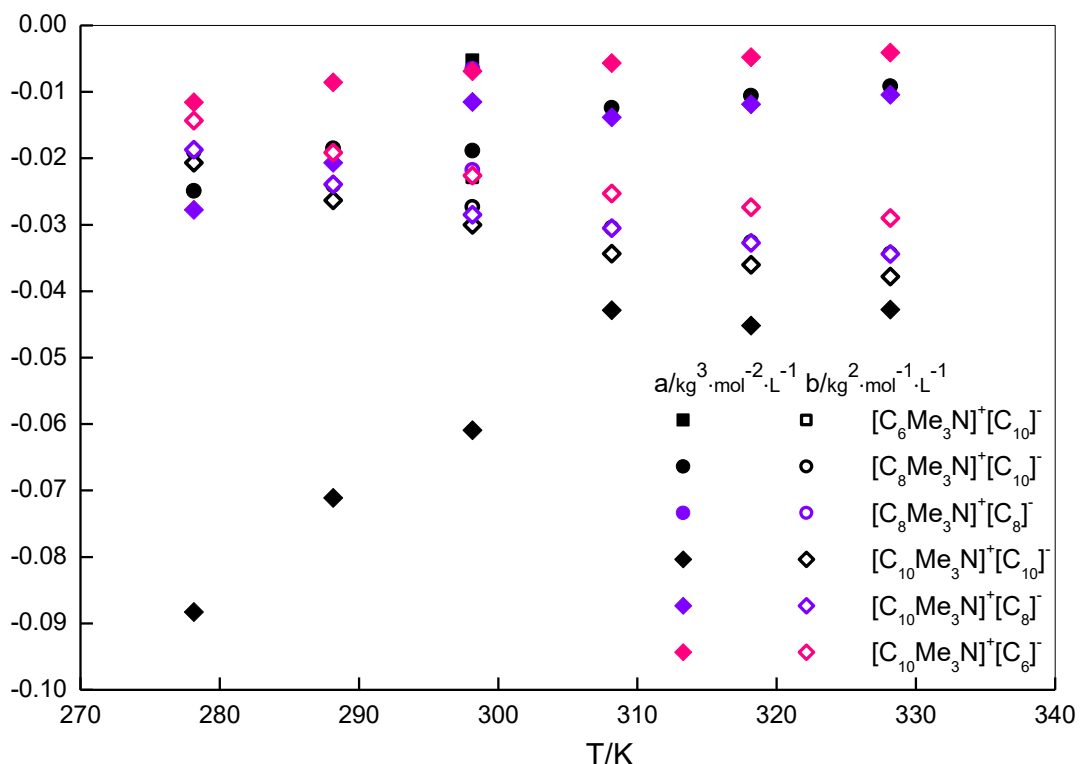
Calculation of $n_h^0(S)$

To estimate the maximum number of water molecules around the cation and anion monomers of surfactant in a single layer, $n_h^0(S)$,[2] first the radii of water molecule and surfactant cation and anion are approximated assuming they are spherical from their corresponding molar volume of water, $V_m(H_2O) = 18.069$ cm^3 mol^{-1}, and apparent molar volume of free monomers, V_ϕ^{mon}.

$$r_{mon} = \sqrt[3]{\frac{3V_\phi^{mon}}{8\pi N_A}} \; ; \qquad r_w = \sqrt[3]{\frac{3V_m(H_2O)}{4\pi N_A}}$$

(ii)

$n_h^0(S)$ is calculated according to eq iii.

$$n_h^0(S) = 4\pi \left[(r_{mon} + r_w)/r_w \right]^2 / \sqrt{3} \tag{iii}$$

List of the symbols used in the data analysis

General

c	total molar surfactant concentration
m	total surfactant concentration in mol per kg of solution
b	total surfactant molality (mol per kg of solvent)
m_{sol}	mass of solvent (water)
n_S	total amount of surfactant
T	temperature
R	molar gas constant
M	molar mass
ρ	density
V_ϕ	apparent molar volume

Thermodynamics

n_1	aggregation number for the first step in the two-step model
n_2	aggregation number for the second step in the two-step model
$\Delta_{M,1}H^\theta$	standard molar enthalpy of micellization for the first step in the two-step model
$\Delta_{M,2}H^\theta$	standard molar enthalpy of micellization for the second step in the two-step model
$\Delta_{M,1}G^\theta$	standard molar Gibbs free energy of micellization for the first step in the two-step model
$\Delta_{M,2}G^\theta$	standard molar Gibbs free energy of micellization for the second step in the two-step model
$\Delta_{M,1}S^\theta$	standard molar entropy of micellization for the first step in the two-step model
$\Delta_{M,2}S^\theta$	standard molar entropy of micellization for the second step in the two-step model
$\Delta_{M,1}c_p{}^\theta$	standard molar heat capacity change upon micellization for the first step in the two-step model
$\Delta_{M,2}c_p{}^\theta$	standard molar heat capacity change upon micellization for the second step in the two-step model
C^+	cations
A^-	anions
$C_{n_1}A_{\beta n_1}$	micelles with aggregation number n_1 (first step)
$C_{n_2}A_{\beta n_2}{}^{(1-\beta)n_2+}$	micelles with aggregation number n_2 (second step)
β	the fraction of (in micelle) incorporated co-ions (for the second step in the two step model)
$K_{M,1}$	apparent equilibrium of the first step
$K_{M,2}$	apparent equilibrium of the second step
n_{sol}	amount of solvent (water)
n_C	amount of cations
n_A	amount of anions
$n_{M,1}$	amount of micelles with aggregation number n_1 (first step)
$n_{M,2}$	amount of micelles with aggregation number n_2 (second step)
x_C	molar fraction of cations

x_A	molar fraction of anions
$x_{M,1}$	molar fraction of micelles with aggregation number n_1 (first step)
$x_{M,2}$	molar fraction of micelles with aggregation number n_2 (second step)
$\sum n_i$	sum of amounts of species
H	enthalpy of solution; enthalpy of solution after addition
H_0	enthalpy of solution before addition
H_{stock}	enthalpy of stock solution
$\overline{H}_{sol}$	partial molar enthalpy of solvent (water)
$\overline{H}_C$	partial molar enthalpy of cations
$\overline{H}_A$	partial molar enthalpy of anions
$\overline{H}_{M,1}$	partial molar enthalpy of micelles with aggregation number n_1 (first step)
$\overline{H}_{M,2}$	partial molar enthalpy of micelles with aggregation number n_2 (second step)
$\overline{H}_{CA}$	partial molar enthalpy of cations/anion pairs
$\overline{H}_{MA,2}$	partial molar enthalpy of micelle/couterion pairs for the second step
$\overline{H}_{index}^{\theta}$	standard molar enthalpies
B_{CA}'	temperature derivative of Guggenheim's coefficient B_{CA} for cation/anion pairs
$B_{M,2}'$	temperature derivative of Guggenheim's coefficient $B_{M,2}$ micelle/couterion pairs for the second step
n_{avg}	average aggregation number at a given total concentration of surfactant and temperature
β_{avg}	the fraction of (in micelle) incorporated co-ions at a given total concentration of surfactant and temperature
α	fraction of surfactant in micelle form

DRS

ν	frequency
ε'	relative permittivity
ε''	dielectric loss
τ_j	relaxation time of mode j
S_j	amplitude of mode j
c_{s3}, c_{s4}	molar concentration of water molecules slowed down in their dynamics
$R_{\tau3}, R_{\tau4}$	factor by which water molecules are slowed down in their dynamics
Z_{s3}, Z_{s4}	number of water molecules per ion of surfactant slowed down in their dynamics
c_b	bulk water concentration determined from modes 5 and 6
c_w	analytical water concentration
Z_t	effective total hydration number of surfactant in solution
Z^{mon}	number of water molecules per monomer of free surfactant slowed down in their dynamics
Z_{s3}^M, Z_{s4}^M	number of water molecules per ion pair of surfactant in a micelle slowed down in their dynamics
Z_t^M	effective total hydration number of a micelle per ion pair of surfactant

Thermodynamics of micellization

Calculating amounts of species at given total concentration of surfactant

Two-step micellization model in the case of positively charged micelles can be represented with two equilibra

$$n_1 C^+ + n_1 A^- \xrightleftharpoons{K_{M,1}} C_{n_1} A_{n_1} \tag{iv}$$

$$n_2 C^+ + \beta n_2 A^- \xrightleftharpoons{K_{M,2}} C_{n_2} A_{\beta n_2}{}^{(1-\beta)n_2+} \tag{v}$$

where C^+ represents the free cations, A^- the corresponding free anions, and $C_{n_1}A_{n_1}$ and $C_{n_2}A_{\beta n_2}{}^{(1-\beta)n_2+}$ stand for the micelles (M,1 and M,2) with aggregation numbers n_1 and n_2. The first step micelles are neutral while the second step includes the fraction of (in micelle) incorporated co-ions, β. If the micelles are negatively charged the anion and cation exchange roles thus the same model can be applied in both cases keeping in mind the reverse role of the cation and anion. The equilibria between the involved species can be expressed by apparent equilibrium constants, K_{M1} and K_{M2},

$$K_{M,1} = \frac{a_{M,1}}{a_C^{n_1} a_A^{n_1}} = \frac{x_{M,1}}{x_C^{n_1} x_A^{n_1}} K_{\gamma,1}; \quad K_{M,2} = \frac{a_{M,2}}{a_C^{n_2} a_A^{\beta n_2}} = \frac{x_{M,2}}{x_C^{n_2} x_A^{\beta n_2}} K_{\gamma,2} \tag{vi}$$

where activities are approximated by the molar fractions of species assuming $K_{\gamma,1} = 1$ and $K_{\gamma,2} = 1$. The values for $K_{M,1}$ and $K_{M,2}$ are obtained from standard molar Gibbs free energies of micellization, $\Delta_{M,1}G^\theta$ and $\Delta_{M,2}G^\theta$,

$$\Delta_{M,1}G^\theta = -\frac{RT}{n_1} \ln K_{M,1}; \Delta_{M,2}G^\theta = -\frac{RT}{n_2} \ln K_{M,2} \tag{vii}$$

and determine composition of each species at given total concentration of surfactant, c. Knowing the total mass, m, and density, ρ, of solution, mass of solvent, m_{sol}, is calculated fallowed by amount of solvent, n_{sol}, and total amount of surfactant, n_S, from the molar mass of solvent and surfactant. Introducing the sum of amounts of species, $\sum n_i$,

$$\sum n_i = n_{sol} + 2 n_S + \left(1 - 2n_1\right)n_{M,1} + \left(1 - \left(1+\beta\right)n_2\right)n_{M,2} \tag{viii}$$

the amounts of free cations, n_C,

$$n_C = n_S - n_1 n_{M,1} - n_2 n_{M,2} \tag{ix}$$

and free anions, n_A,

$$n_A = n_S - n_1 n_{M,1} - \beta n_2 n_{M,2} \tag{x}$$

enables the transformation of eq vi into two equations

$$K_{M,1} = \frac{n_{M,1}\left(n_{sol} + 2n_S + \left(1 - 2n_1\right)n_{M,1} + \left(1 - \left(1+\beta\right)n_2\right)n_{M,2}\right)^{2n_1 - 1}}{\left(n_S - n_1 n_{M,1} - n_2 n_{M,2}\right)^{n_1}\left(n_S - n_1 n_{M,1} - \beta n_2 n_{M,2}\right)^{n_1}} \tag{xi}$$

$$K_{M,2} = \frac{n_{M,2}\left(n_{sol} + 2n_S + \left(1 - 2n_1\right)n_{M,1} + \left(1 - \left(1+\beta\right)n_2\right)n_{M,2}\right)^{(1+\beta)n_2 - 1}}{\left(n_S - n_1 n_{M,1} - n_2 n_{M,2}\right)^{n_2}\left(n_S - n_1 n_{M,1} - \beta n_2 n_{M,2}\right)^{\beta n_2}} \tag{xii}$$

with two unknown variables, $n_{M,1}$ and $n_{M,2}$. This system of two equations cannot be solved analytically. Therefore, the tangent method was used to find the solution numerically.

Enthalpy of solution

Knowing all the amounts of species in added titrant and cell before and after its addition theoretical enthalpy of solution is calculated. Enthalpy of solution can be defined in two ways: with enthalpies of ions

$$H = n_{sol}\overline{H}_{sol} + n_C\overline{H}_C + n_A\overline{H}_A + n_{M,1}\overline{H}_{M,1} + n_{M,2}\overline{H}_{M,2} \qquad (xiii)$$

and enthalpies of ion pairs

$$H = n_{sol}\overline{H}_{sol} + n_{CA}\overline{H}_{CA} + n_{M,1}\overline{H}_{M,1} + n_{MA,2}\overline{H}_{MA,2} \qquad (xiv)$$

where indexes "sol", "CA" and "MA,2" denote solvent, surfactant monomers in form of ion pairs and micelle/counterion pairs respectively. Although the enthalpies of ion pairs are different from the values for ions, the amount of the free cations, n_C, is equal to amount of cation/anion pairs, n_{CA}, and the amount of micelles, $n_{M,2}$, is equal to amount of cation/micelle pairs, $n_{MA,2}$. Thus, defining enthalpy of solution with ion pairs is only required to introduce Guggenheim approximation[3] which is used to calculate enthalpies of ion pairs

$$\overline{H}_{CA} = \overline{H}_{CA}^{\theta} + 2RT^2 B'_{CA}b_{CA} \qquad (xv)$$

$$\overline{H}_{MA,2} = \overline{H}_{MA,2}^{\theta} + \left(1 + (1-\beta)n_2\right)RT^2 B'_{M,2}b_{MA,2} \qquad (xvi)$$

in which B_{CA}' and $B_{M,2}'$ are the temperature derivatives of Guggenheim's coefficients B_{CA} and $B_{M,2}$, whereas, b_{CA} and $b_{M,2}$ are molalities of surfactant in the form of ion pairs of free monomers with counterions and of micelles with counterions, respectively. This correction is required to account for the enthalpy of dilution (slopes of the curves before and after cmc). In the enthalpogram this is most noticeable below cmc where the curve without this correction would be flat as is often the case for non-ionic surfactants. By combining standard molar enthalpies of micellization, $\Delta_{M,1}H^{\theta}$ and $\Delta_{M,2}H^{\theta}$,

$$\Delta_{M,1}H^{\theta} = \frac{1}{n_1}\overline{H}_{MA,1}^{\theta} - \overline{H}_{CA}^{\theta} \qquad (xvii)$$

$$\Delta_{M,2}H^{\theta} = \frac{1}{n_2}\overline{H}_{MA,2}^{\theta} - \overline{H}_{CA}^{\theta} \qquad (xviii)$$

with eqs xiv-xvi the enthalpy of solution is obtained

$$H = n_{sol}\overline{H}_{sol} + n_S\overline{H}_{CA}^{\theta} + n_1 n_{M,1}\Delta_{M,1}H^{\theta} + n_2 n_{M,2}\Delta_{M,2}H^{\theta} + 2RT^2 B'_{CA}b_C n_C + \\ RT^2\left(1 + (1-\beta)n_2\right)B'_{M,2}b_{M,2}n_{M,2} \qquad (xix)$$

which can be applied in micellization studies by any calorimetric experimental method.

ITC enthalpy change

Heat changes measured with ITC are contributions of three enthalpies divided by the total surfactant amount added, $n_{S,stock}$;

$$\Delta H = \frac{q}{n_{S,stock}} = \frac{H - H_0 - H_{stock}}{n_{S,stock}} \tag{xx}$$

enthalpy of stock solution, H_{stock}, and enthalpies of solution in cell before, H_0, and after addition, H. By using eq xx for each enthalpy and combining it with eq xxi, heat change after an addition of stock solution can be expressed as

$$\Delta H = \frac{n_{sol} - n_{sol,0} - n_{sol,stock}}{n_{S,stock}} \overline{H}^{\theta}_{sol} + \frac{n_S - n_{S,0} - n_{S,stock}}{n_{S,stock}} \overline{H}^{\theta}_{CA} +$$

$$n_1 \frac{n_{M,1} - n_{M,1,0} - n_{M,1,stock}}{n_{S,stock}} \Delta_{M,1} H^{\theta} + n_2 \frac{n_{M,2} - n_{M,2,0} - n_{M,2,stock}}{n_{S,stock}} \Delta_{M,2} H^{\theta} + \tag{xxi}$$

$$RT^2 \left(\begin{array}{l} 2B'_{CA} \dfrac{b_C n_C - b_{C,0} n_{C,0} - b_{C,stock} n_{C,stock}}{n_{S,stock}} + \\[2em] \left(1 + (1-\beta) n_2 \right) B'_{M,2} \dfrac{b_{M,2} n_{M,2} - b_{M,2,0} n_{M,2,0} - b_{M,2,stock} n_{M,2,stock}}{n_{S,stock}} \end{array} \right)$$

First two terms in eq xx are equal to zero because total amount of solvent and surfactant in the titration cell after the addition is the same as sum of amounts before the addition and the addition itself. Replacing molalities, b_i, by

$$b_i = \frac{n_i}{m_{sol}} \tag{xxii}$$

and defining the changes in amount of micelles, $\Delta n_{M,1}/\Delta n$ and $\Delta n_{M,2}/\Delta n$, as

$$\frac{\Delta n_{M,1}}{\Delta n} = n_1 \frac{n_{M,1} - n_{M,1,0} - n_{M,1,stock}}{n_{S,stock}} \tag{xxiii}$$

$$\frac{\Delta n_{M,2}}{\Delta n} = n_2 \frac{n_{M,2} - n_{M,2,0} - n_{M,2,stock}}{n_{S,stock}} \tag{xxiv}$$

eq xxii reduces into its final form

$$\Delta H = \frac{\Delta n_{M,1}}{\Delta n} \Delta_{M,1} H^{\theta} + \frac{\Delta n_{M,2}}{\Delta n} \Delta_{M,2} H^{\theta} + \frac{RT^2}{n_{S,stock}} 2B'_{CA} \left(\frac{n_C^2}{m_{sol}} - \frac{n_{C,0}^2}{m_{sol,0}} - \frac{n_{C,stock}^2}{m_{sol,stock}} \right) +$$

$$\frac{RT^2}{n_{S,stock}} B'_{M,2} \left(1 + (1-\beta) n_2 \right) \left(\frac{n_{M,2}^2}{m_{sol}} - \frac{n_{M,2,0}^2}{m_{sol,0}} - \frac{n_{M,2,stock}^2}{m_{sol,stock}} \right) \tag{xxv}$$

Global analysis

In the global analysis of ITC experiments the Kirchoff's law

$$\Delta_{M,1}H^{\theta} = \Delta_{M,1}H^{\theta}_{T_r} + \Delta_{M,1}c_p^{\theta}(T\text{-}T_r) \tag{xxvi}$$

$$\Delta_{M,2}H^{\theta} = \Delta_{M,2}H^{\theta}_{T_r} + \Delta_{M,2}c_p^{\theta}(T\text{-}T_r) \tag{xxvii}$$

and the integrated Gibbs-Helmholtz equation

$$\Delta_{M,1}G^{\theta} = T\left[\Delta_{M,1}G^{\theta}_{T_r}/T_r + \Delta_{M,1}H^{\theta}_{T_r}(1/T - 1/T_r) + \Delta_{M,1}c_p^{\theta}(1 - T_r/T - \ln(T/T_r))\right] \tag{xxviii}$$

$$\Delta_{M,2}G^{\theta} = T\left[\Delta_{M,2}G^{\theta}_{T_r}/T_r + \Delta_{M,2}H^{\theta}_{T_r}(1/T - 1/T_r) + \Delta_{M,2}c_p^{\theta}(1 - T_r/T - \ln(T/T_r))\right] \tag{xxix}$$

are used, where $\Delta_{M,1}G_{Tr}^{\theta}$ and $\Delta_{M,2}G_{Tr}^{\theta}$ are the standard Gibbs free energy and $\Delta_{M,1}H_{Tr}^{\theta}$ and $\Delta_{M,2}H_{Tr}^{\theta}$ are the standard molar enthalpy of micellization at reference temperature T_r for steps 1 and 2. Standard molar heat capacities of micellization for first and second step, $\Delta_{M,1}c_p^{\theta}$ and $\Delta_{M,2}c_p^{\theta}$, were taken as temperature independent in the examined temperature range because the attempt to introduce their linear dependence on temperature has resulted in less temperature dependence than the inaccuracy of reference values themselves. Moreover, B_{CA}' and $B_{M,2}'$ were assumed to be linearly depended with temperature introducing

$$B_{CA,T}' = B_{CA,T_r}' + B_{CA}''(T\text{-}T_r) \tag{xxx}$$

$$B_{M,2,T}' = B_{M,2,T_r}' + B_{M,2}''(T\text{-}T_r) \tag{xxxi}$$

B_{CA}'' and $B_{M,2}''$ as the slopes and $B_{CA,Tr}'$ and $B_{M,2,Tr}'$ values at reference temperature T_r. From the eqs vi, xxvi and xxvii-xxxiii it is evident that the ITC model equations may be described in terms of n_1, n_2, β, $\Delta_{M,1}G_{Tr}^{\theta}$, $\Delta_{M,2}G_{Tr}^{\theta}$, $\Delta_{M,1}H_{Tr}^{\theta}$, $\Delta_{M,2}H_{Tr}^{\theta}$, $\Delta_{M,1}c_p^{\theta}$, $\Delta_{M,2}c_p^{\theta}$, and the coefficients $B_{CA,Tr}'$, $B_{M,2,Tr}'$, B_{CA}'', and $B_{M,2}''$ at any surfactant concentration, c, and temperature, T. All these values were obtained by fitting of the model equation to the experimental data points in the following manner. The model equation was compared to the experimental curves via the χ^2 function defined as

$$\chi^2 = \sum_T f_T \sum_i \left(\Delta H_i - \Delta H_i^{mod}\right)^2 \tag{xxxii}$$

where ΔH_i and ΔH_i^{mod} represent the experimental and the model enthalpy, whereas f_T represents the correction factor which differs from 1 if error of experimental points at temperature T is significantly greater. By minimization of χ^2 function best-fit values of the above-mentioned global parameters were calculated using modified Simplex method which was ran at least 100 times each time from randomly generated starting set of parameters. Values of global parameters were further used to calculate corresponding parameters for each temperature. The standard molar entropy of micellization, $\Delta_{M,1}S^{\theta}$ and $\Delta_{M,2}S^{\theta}$, associated with the examined process was obtained from the Gibbs-Helmholtz equation.

$$\Delta_{M,1}S^{\theta} = \frac{\Delta_{M,1}H^{\theta} - \Delta_{M,1}G^{\theta}}{T} \tag{xxxiii}$$

$$\Delta_{M,2}S^{\theta} = \frac{\Delta_{M,2}H^{\theta} - \Delta_{M,2}G^{\theta}}{T} \tag{xxxiv}$$

Modification of the model for the introduction of the bilayer structure

In the case of $[C_{10}Me_3N]^+[C_{10}]^-$ first step was best fitted by a very low aggregation number (1.5) yet the best fit also revealed low heat capacity change making formation of dimers and trimers an unlikely explanation. Therefore, the assumption of the formation of bilayers was proposed. This is achieved by fixing n_1 in eq iv to 1. Additionally the activity coefficient of bilayer phase should no longer be assumed to be approximately equal to molar fraction. Therefore, the coefficient A is introduced

$$K_{M,1} = K_B = \frac{x_B \gamma_B}{x_C x_A}; \quad \gamma_B = \frac{1}{a_M^A} = \left(\frac{n_S}{n_2 n_{M,2}} \right)^A \qquad \text{(xxxv)}$$

which ensures that unlike in the case of the dimer, the formation of bilayers is pre-dependent on the formation of aggregates. This has a limited effect on the resulting thermodynamics parameters and could be neglected.

Isothermal titration calorimetry (ITC)
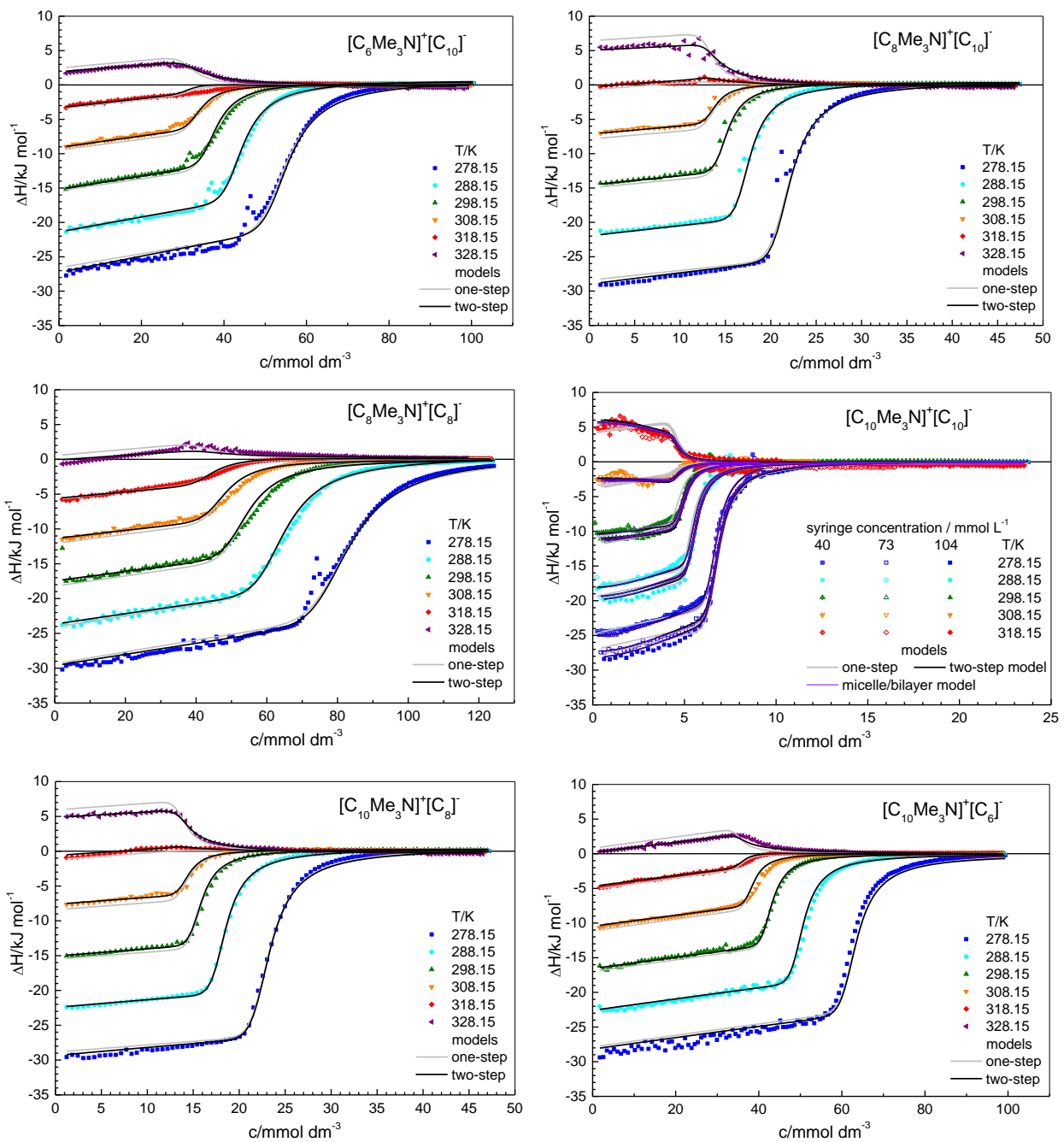
Figure S5. Enthalpograms of $[C_xMe_3N]^+[C_y]^-$. Solid lines represent the fit according to the one-step (gray) and the two-step model (black) and micelle/bilayer model (purple) for $[C_{10}Me_3N]^+[C_{10}]^-$.

Table S3. Thermodynamic parameters of micellization for investigated systems in water at all the investigated temperatures for both steps: Standard molar Gibbs free energies, $\Delta_{M,1}G^{\theta}$ and $\Delta_{M,2}G^{\theta}$, enthalpies, $\Delta_{M,1}H^{\theta}$ and $\Delta_{M,2}H^{\theta}$, entropies, $\Delta_{M,1}S^{\theta}$ and $\Delta_{M,2}S^{\theta}$, of micellization, coefficients B_{CA}' and $B_{M,2}'$ (eqs xii-xiv) and critical micelle concentration, cmc, in water as obtained for the second step by the fitting procedure.[a]

T	$\Delta_{M,1}G^{\theta}$	$\Delta_{M,1}H^{\theta}$	$\Delta_{M,1}S^{\theta}$	$\Delta_{M,2}G^{\theta}$	$\Delta_{M,2}H^{\theta}$	$\Delta_{M,2}S^{\theta}$	B_{CA}'	$B_{M,2}'$	cmc
$[C_6Me_3N]^+[C_{10}]^-$
278.15	-29.1 ± 0.3	30.2 ± 1	213	-27.9 ± 0.3	31.3 ± 0.8	213	0.047 ± 0.003	-0.52 ± 0.08	54 ± 1
288.15	-31.1 ± 0.3	24.3 ± 1	192	-29.9 ± 0.3	23.8 ± 0.7	186	0.040 ± 0.003	-0.39 ± 0.08	44 ± 1
298.15	-33.0 ± 0.3	18.3 ± 1	172	-31.6 ± 0.4	16.2 ± 0.6	160	0.033 ± 0.003	-0.26 ± 0.08	37 ± 1
308.15	-34.6 ± 0.3	12.4 ± 1	152	-33.1 ± 0.4	8.7 ± 0.6	136	0.026 ± 0.003	-0.14 ± 0.08	34 ± 1
318.15	-36.0 ± 0.3	6.5 ± 1	134	-34.3 ± 0.4	1.2 ± 0.8	112	0.020 ± 0.003	-0.02 ± 0.08	32 ± 1
328.15	-37.3 ± 0.3	0.6 ± 1	115	-35.3 ± 0.4	-6.3 ± 0.8	88	0.013 ± 0.003	0.11 ± 0.08	32 ± 1
$[C_8Me_3N]^+[C_{10}]^-$
278.15	-32.7 ± 0.4	32.6 ± 2	235	-32.2 ± 0.5	32.0 ± 0.4	231	0.064 ± 0.006	-0.44 ± 0.04	21.5 ± 0.5
288.15	-35.0 ± 0.4	26.4 ± 2	213	-34.3 ± 0.5	23.8 ± 0.4	202	0.055 ± 0.006	-0.36 ± 0.04	17.3 ± 0.5
298.15	-37.0 ± 0.4	20.2 ± 2	192	-36.2 ± 0.5	15.6 ± 0.4	174	0.047 ± 0.006	-0.29 ± 0.04	14.7 ± 0.5
308.15	-38.8 ± 0.4	14.0 ± 2	171	-37.8 ± 0.5	7.4 ± 0.4	147	0.037 ± 0.006	-0.21 ± 0.04	13.5 ± 0.5
318.15	-40.4 ± 0.4	7.8 ± 2	152	-39.2 ± 0.5	-0.8 ± 0.4	121	0.028 ± 0.006	-0.14 ± 0.04	13.5 ± 0.5
328.15	-41.9 ± 0.4	1.6 ± 2	132	-40.2 ± 0.5	-9.0 ± 0.4	95	0.019 ± 0.006	-0.06 ± 0.04	12.9 ± 0.5
$[C_8Me_3N]^+[C_8]^-$
278.15	-27.0 ± 0.4	34.9 ± 1.1	222	-25.8 ± 0.8	34.4 ± 0.8	216	0.032 ± 0.005	-0.53 ± 0.15	82 ± 3
288.15	-29.1 ± 0.4	28.0 ± 1.0	198	-27.8 ± 0.8	25.6 ± 0.8	185	0.027 ± 0.005	-0.30 ± 0.10	62 ± 1
298.15	-31.0 ± 0.4	21.2 ± 0.7	175	-29.5 ± 0.8	16.7 ± 1.0	155	0.023 ± 0.005	-0.06 ± 0.07	52 ± 1
308.15	-32.6 ± 0.4	14.4 ± 0.5	153	-30.9 ± 0.8	7.9 ± 1.0	126	0.019 ± 0.005	0.17 ± 0.08	47 ± 1
318.15	-34.0 ± 0.4	7.6 ± 0.5	131	-32.0 ± 0.8	-1.0 ± 1.2	98	0.014 ± 0.005	0.40 ± 0.15	44 ± 1
328.15	-35.2 ± 0.4	0.7 ± 0.6	110	-32.8 ± 0.8	-9.8 ± 1.5	70	0.010 ± 0.005	0.64 ± 0.25	43 ± 1

[a]Units: T, K; $\Delta_M G^{\theta}$, $\Delta_M H^{\theta}$, kJ·mol^{-1}; $\Delta_M S^{\theta}$, J·K^{-1}·mol^{-1}; B_S', $B_{M,2}'$, kg·K^{-1}·mol^{-1}; cmc, mmol·dm^{-3}

Table S3. continued

T	$\Delta_{M,1}G^\theta$	$\Delta_{M,1}H^\theta$	$\Delta_{M,1}S^\theta$	$\Delta_{M,2}G^\theta$	$\Delta_{M,2}H^\theta$	$\Delta_{M,2}S^\theta$	B_{CA}'	$B_{M,2}'$	cmc
$[C_{10}Me_3N]^+[C_{10}]^-$ [b]									
278.15	-14.8 ± 0.9	31 ± 6	166	-38.4 ± 1.2	29.5 ± 0.9	244	0.08 ± 0.05	-0.4 ± 0.3	6.6 ± 0.2
288.15	-16.3 ± 0.8	20 ± 5	128	-40.7 ± 1.2	20.6 ± 0.7	213	0.07 ± 0.05	-0.1 ± 0.3	5.5 ± 0.2
298.15	-17.4 ± 0.7	8 ± 4	90	-42.7 ± 1.2	11.7 ± 0.5	182	0.06 ± 0.05	0.1 ± 0.3	4.9 ± 0.2
308.15	-18.1 ± 0.7	-3 ± 4	54	-44.3 ± 1.2	2.8 ± 0.6	153	0.06 ± 0.05	0.4 ± 0.3	4.8 ± 0.2
318.15	-18.5 ± 0.8	-14 ± 6	19	-45.7 ± 1.2	-6.1 ± 0.8	125	0.05 ± 0.05	0.6 ± 0.3	4.7 ± 0.2
$[C_{10}Me_3N]^+[C_8]^-$									
278.15	-32.8 ± 0.6	32.8 ± 2.0	236	-32.2 ± 0.4	32.5 ± 0.4	232	0.046 ± 0.009	-0.39 ± 0.1	22.8 ± 0.3
288.15	-35.0 ± 0.6	26.6 ± 1.5	214	-34.3 ± 0.5	24.3 ± 0.4	204	0.041 ± 0.009	-0.35 ± 0.1	18.3 ± 0.3
298.15	-37.1 ± 0.6	20.4 ± 1.5	193	-36.2 ± 0.6	16.2 ± 0.4	176	0.036 ± 0.009	-0.30 ± 0.1	15.7 ± 0.3
308.15	-38.9 ± 0.6	14.2 ± 1.5	172	-37.9 ± 0.6	8.0 ± 0.4	149	0.031 ± 0.009	-0.25 ± 0.1	14.0 ± 0.5
318.15	-40.5 ± 0.5	8.0 ± 1.5	153	-39.2 ± 0.6	-0.1 ± 0.4	123	0.027 ± 0.009	-0.21 ± 0.1	14.0 ± 0.5
328.15	-41.9 ± 0.4	1.8 ± 1.5	133	-40.3 ± 0.5	-8.3 ± 0.5	98	0.022 ± 0.009	-0.16 ± 0.1	13.9 ± 0.5
$[C_{10}Me_3N]^+[C_6]^-$									
278.15	-29.1 ± 0.5	35.0 ± 2.0	230	-28.9 ± 0.5	32.4 ± 0.5	220	0.033 ± 0.004	-0.69 ± 0.1	62 ± 1
288.15	-31.2 ± 0.4	28.7 ± 1.8	208	-31.0 ± 0.5	25.3 ± 0.5	195	0.031 ± 0.003	-0.56 ± 0.1	50 ± 1
298.15	-33.2 ± 0.4	22.4 ± 1.5	187	-32.8 ± 0.5	18.3 ± 0.5	171	0.028 ± 0.003	-0.43 ± 0.1	43 ± 1
308.15	-35.0 ± 0.4	16.1 ± 1.5	166	-34.4 ± 0.5	11.2 ± 0.5	148	0.026 ± 0.003	-0.29 ± 0.1	38 ± 1
318.15	-36.5 ± 0.3	9.8 ± 1.5	146	-35.8 ± 0.4	4.1 ± 0.5	126	0.023 ± 0.003	-0.16 ± 0.1	36 ± 1
328.15	-37.9 ± 0.3	3.5 ± 1.5	126	-36.9 ± 0.4	-2.9 ± 0.5	104	0.021 ± 0.004	-0.02 ± 0.1	35 ± 1

[a]Units: T, K; $\Delta_M G^\theta$, $\Delta_M H^\theta$, kJ·mol^{-1}; $\Delta_M S^\theta$, J·K^{-1}·mol^{-1}; B_{CA}', $B_{M,2}'$, kg·K^{-1}·mol^{-1}; cmc, mmol·dm^{-3}
[b]Bilayer structure; coefficient $A = 0.03 ± 0.02$

Table S4. Aggregation numbers, n_1 and n_2, as defined in eq iv, combined aggregation numbers of cations and anions, $n_{agg,1}$ and $n_{agg,2}$, standard molar heat capacities of micellization, $\Delta_{M,1}c_p^\theta$ and $\Delta_{M,2}c_p^\theta$, for both steps, fraction of (in micelle) incorporated co-ions for the second step, β, and second temperature derivatives, B_{CA}'', and $B_{M,2}''$, (eqs xxviii and xxix) for investigated systems in water as obtained by the fitting procedure of the two-step micellization model.[a]

	n_1	$n_{agg,1}$	$\Delta_{M,1}c_p^\theta$	β	n_2	$n_{agg,2}$	$\Delta_{M,2}c_p^\theta$	B_{CA}''	$B_{M,2}''$
$[C_6Me_3N]^+[C_{10}]^-$	11 ± 2	21 ± 4	-590 ± 40	0.88 ± 0.03	14 ± 2	27 ± 4	-750 ± 40	-0.6 ± 0.2	12 ± 10
$[C_8Me_3N]^+[C_{10}]^-$	11 ± 2	22 ± 4	-620 ± 70	0.89 ± 0.02	15 ± 1	29 ± 2	-820 ± 30	-0.9 ± 0.3	7 ± 4
$[C_8Me_3N]^+[C_8]^-$	9 ± 1	18 ± 2	-680 ± 40	0.87 ± 0.07	13 ± 2	23 ± 4	-880 ± 40	-0.4 ± 0.2	23 ± 9
$[C_{10}Me_3N]^+[C_{10}]^-$	1.5 ± 1.5	3 ± 3	-900 ± 200	0.99 ± 0.20	19 ± 3	38 ± 6	-920 ± 100	-0.7 ± 0.7	25 ± 20
	1^b	2^b	-1100 ± 100	0.92 ± 0.06	18 ± 2	36 ± 4	-890 ± 30	-0.7 ± 0.7	25 ± 15
$[C_{10}Me_3N]^+[C_8]^-$	12 ± 1	25 ± 2	-620 ± 70	0.89 ± 0.02	16 ± 1	31 ± 2	-820 ± 30	-0.5 ± 0.4	7 ± 5
$[C_{10}Me_3N]^+[C_6]^-$	18 ± 2	36 ± 4	-630 ± 60	0.93 ± 0.03	23 ± 3	44 ± 6	-710 ± 20	-0.2 ± 0.2	13 ± 9

[a]Units: $\Delta_M c_p^\theta$, J·K^{-1}·mol^{-1}; B_{CA}'', $B_{M,2}''$, g·K^{-2}·mol^{-1}
[b]Fixed to represent bilayer structure
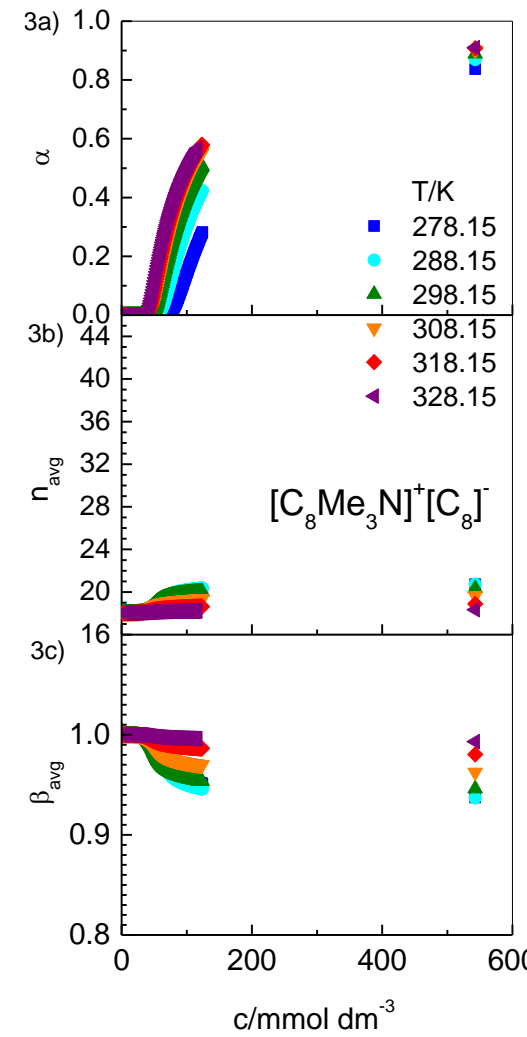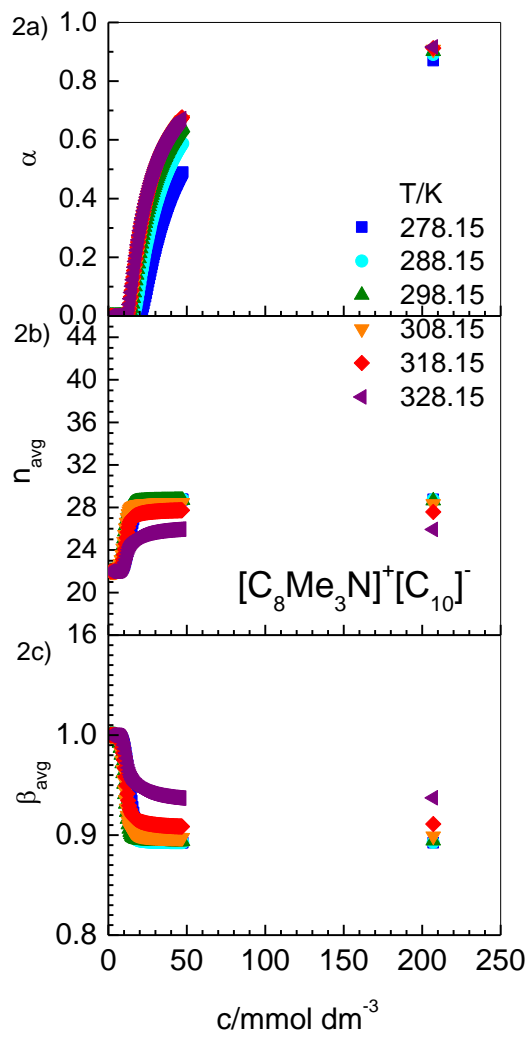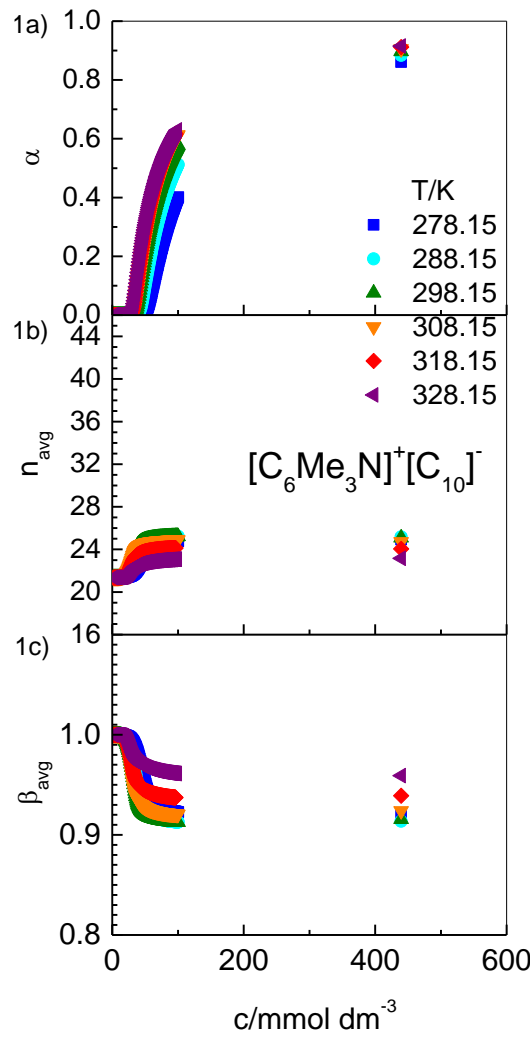
Figure S6. Concentration dependence of a) fraction of surfactant ions bound in micelles, α, b) the average aggregation number, n_{avg}, and c) the average fraction of incorporated co-ions, β_{avg}, for 1) $[C_6Me_3N]^+[C_{10}]^-$, 2) $[C_8Me_3N]^+[C_{10}]^-$ and 3) $[C_8Me_3N]^+[C_8]^-$ at investigated temperatures as estimated by using eqs 12-14.
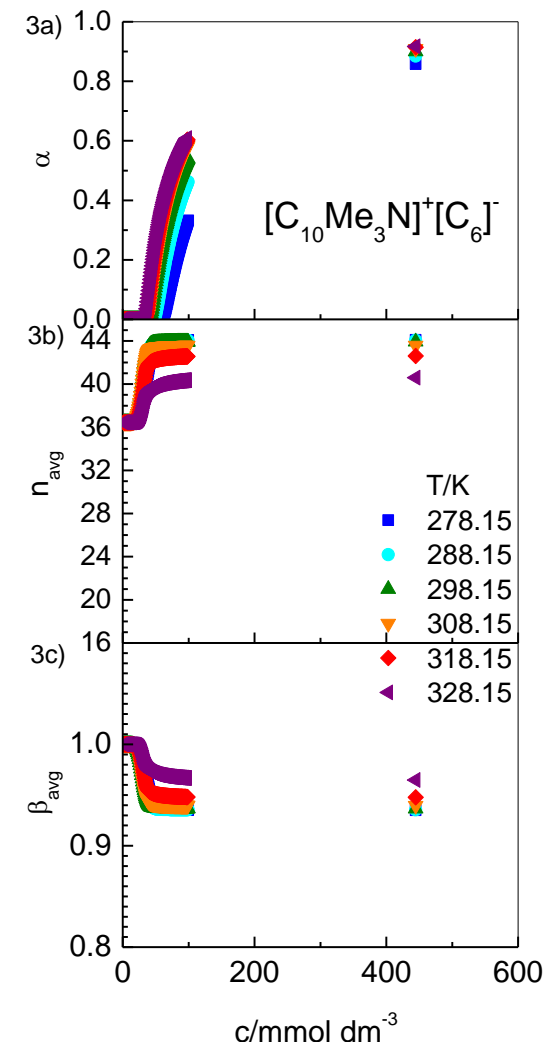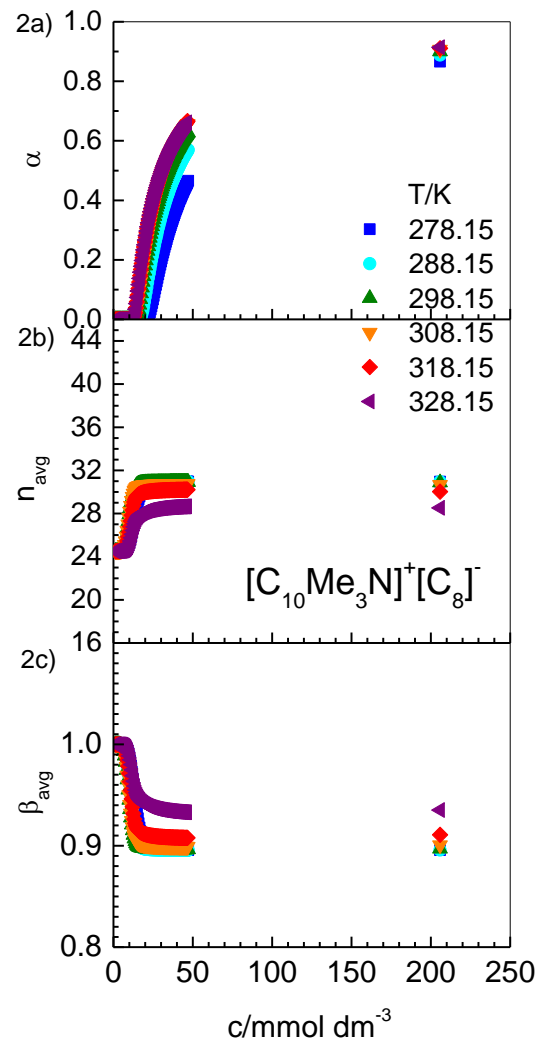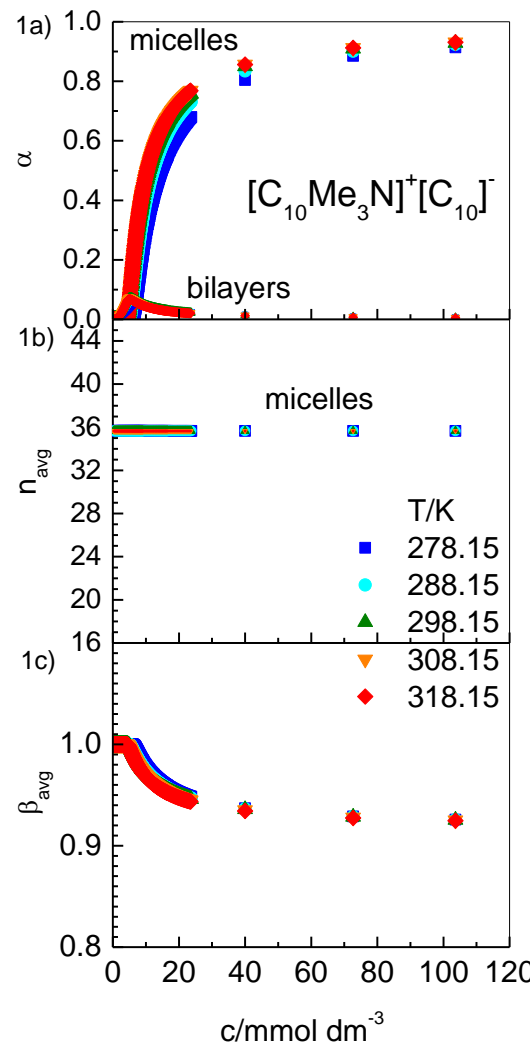
Figure S7. Concentration dependence of a) fraction of surfactant ions bound in micelles, α, b) the average aggregation number, n_{avg}, and c) the average fraction of incorporated co-ions, β_{avg}, for 1) $[C_{10}Me_3N]^+[C_{10}]^-$, 2) $[C_{10}Me_3N]^+[C_8]^-$ and 3) $[C_{10}Me_3N]^+[C_6]^-$ at investigated temperatures as estimated by using eqs 12-14.

Water accessible surface area (WASA)

$$\Delta_M c_p^\theta(\text{th}) = a \cdot \Delta A_{np} + b \cdot \Delta A_p \qquad\qquad (\text{xxxvi})$$

In the literature, a variety of values for a and b coefficients may be found,[4,5] but in many applications for proteins[5], they give very similar results. Assuming $a = (-1.34 \pm 0.33)$ J·mol^{-1}·K^{-1} Å^{-2} for this coefficient[6] in eq. xxxvi, the values of $\Delta_M c_p^\theta(\text{th})$ in Table S7 are obtained.

Table S5. Loss of water accessible nonpolar surface, ΔA_{np}, and theoretical values of the heat capacity change upon micellization, $\Delta_M c_p^\theta(\text{th})$, in dependence of the number of carbon atoms in the alkyl chain, n.[a]

n	ΔA_{np}	$\Delta_M c_p^\theta(\text{th})$
2	118	-158 ± 39
3	148	-198 ± 49
4	178	-239 ± 59
5	208	-279 ± 69
6	238	-319 ± 79
7	268	-359 ± 88
8	298	-399 ± 98
9	328	-440 ± 108
10	358	-480 ± 118
11	388	-520 ± 128
12	418	-560 ± 138
13	448	-600 ± 148
14	478	-641 ± 158
15	508	-681 ± 168

[a]Units: ΔA_{np}, Å^2; $\Delta_M c_p^\theta$, J·K^{-1}·mol^{-1}

To obtain the theoretical values of the heat capacity change, $\Delta_M c_p^\theta(\text{th})$, for the studied catanionic surfactants both alkyl chains on the cation (n = x) and anion (n = y – 1, one carbon atom forms the -COO$^-$ headgroup) are summed resulting in following values:

	$\Delta_M c_p^\theta(\text{th})$/ J·K^{-1}·mol^{-1}
[C$_6$Me$_3$N]$^+$[C$_{10}$]$^-$	
[C$_8$Me$_3$N]$^+$[C$_8$]$^-$	-759 ± 137
[C$_{10}$Me$_3$N]$^+$[C$_6$]$^-$	
[C$_8$Me$_3$N]$^+$[C$_{10}$]$^-$	
[C$_{10}$Me$_3$N]$^+$[C$_8$]$^-$	839 ± 147
[C$_{10}$Me$_3$N]$^+$[C$_{10}$]$^-$	-920 ± 160

Dielectric relaxation spectroscopy (DRS)

Table S6. Concentrations, c, of the surfactant solutions investigated with DRS and associated relaxation parameters (static permittivity, ε, high-frequency permittivity, ε_∞, amplitudes, S_j, and relaxation times, τ_j, of the resolved modes $j = 1\ldots6$) obtained with the 6D model (5D model for 30 mmol dm^{-3} solutions), densities, ρ, electrical conductivities, κ, and value of the reduced error function, χ^2.[a]

c	ε	ε_∞[b]	S_1	τ_1	S_2	τ_2	S_3	τ_3	S_4	τ_4	S_5	τ_5	S_6	τ_6[b]	ρ	κ	χ^2
$[C_6Me_3N]^+[C_{10}]^-$
29.87	81.10	3.52	1.47	6280			1.73	252	2.15	18.7	68.09	8.14	2.15	0.278	0.996548	0.1215[c]	0.029
74.84	87.14	3.52	3.58	9570	4.08	974	3.04	200	5.86	18.7[b]	64.92	8.14	2.14	0.278	0.995444	0.192[c]	0.037
98.75	87.16	3.52	2.69	5340	6.31	766	3.15	146	3.33	16.0	65.71	8.59	2.46	0.278	0.994812	0.2245	0.019
146.33	90.69	3.52	2.68	4080	10.27	801	4.24	159	4.98	20.6	62.54	8.43	2.46	0.278	0.993558	0.258[c]	0.031
197.55	96.99	3.52	5.30	7040	15.06	821	5.27	146	13.17	15.4	52.57	7.89	2.09	0.278	0.992201	0.310[c]	0.040
247.31	101.40	3.52	6.32	9530	18.72	867	6.63	160	11.56	17.3	52.58	8.06	2.07	0.278	0.990884	0.347[c]	0.048
$[C_8Me_3N]^+[C_{10}]^-$
98.61	88.87	3.52	5.48	2930	5.71	778	3.04	172	1.79	23.9	66.86	8.49	2.48	0.278	0.994094	0.0908	0.043
148.89	96.24	3.52	7.69	5450	10.68	1090	5.02	214	4.44	23.9[b]	62.71	8.24	2.18	0.278	0.992476	0.100[c]	0.028
198.62	100.76	3.52	10.81	4400	13.46	943	6.01	187	4.92	21.9	59.74	8.36	2.31	0.278	0.990870	0.112[c]	0.038
245.84	103.83	3.52	13.10	3620	15.78	855	6.67	169	8.19	17.6	54.34	8.19	2.23	0.278	0.988996	0.123[c]	0.037
$[C_8Me_3N]^+[C_8]^-$
29.88	80.91	3.52	1.67	11360			1.82	199	2.26	17.8	69.05	8.31	2.26	0.278	0.996558	0.100[c]	0.035
75.14	83.75	3.52	2.00[b]	5970	1.87	878	3.78	183	4.96	17.8[b]	65.28	8.36	2.34	0.278	0.995620	0.210[c]	0.021
97.56	85.85	3.52	2.31	5490	4.08	779	4.46	152	3.30	16.0	65.65	8.63	2.52	0.278	0.995031	0.2281	0.023
148.97	90.17	3.52	2.68	2690	8.37	835	5.82	163	4.63	19.1	62.73	8.56	2.41	0.278	0.993662	0.223[c]	0.027
198.28	96.90	3.52	4.56	4350	13.52	914	7.34	172	8.43	18.0	57.46	8.25	2.08	0.278	0.992329	0.228[c]	0.029
247.05	101.68	3.52	6.33	3250	17.21	896	8.54	172	12.15	17.2	51.95	8.02	1.98	0.278	0.991032	0.231[c]	0.036

[a]Units: c, mmol dm^{-3}; τ_j, ps; ρ, kg·dm^{-3}; κ, S m^{-1};
[b]Parameter fixed in the fit.
[c]Estimated from fitting the spectra

Table S6. continued

c	ε	ε_∞[b]	S_1	τ_1	S_2	τ_2	S_3	τ_3	S_4	τ_4	S_5	τ_5	S_6	τ_6[b]	ρ	κ	χ^2
							$[C_{10}Me_3N]^+[C_{10}]^-$										
49.95	84.81	3.52	3.91	6190	3.19	934	1.06	152	5.63	15.4	65.30	8.02	2.20	0.278	0.995259	0.027[c]	0.025
97.31	86.74	3.52	4.62	3580	6.07	752	2.49	123	1.30	16.5[b]	66.21	8.49	2.53	0.278	0.993296	0.0307	0.034
149.54	91.21	3.52	6.78	3800	8.92	926	3.79	183	8.40	16.5	57.54	7.93	2.25	0.278	0.994452	0.040[c]	0.040
198.85	95.89	3.52	8.11	4610	12.57	1100	5.77	212	8.30	18.7	55.45	7.93	2.17	0.278	0.989638	0.046[c]	0.047
246.30	97.80	3.52	9.48	3460	14.37	1050	6.80	209	9.46	18.6	51.99	7.93	2.19	0.278	0.987844	0.054[c]	0.056
							$[C_{10}Me_3N]^+[C_8]^-$										
100.49	88.87	3.52	5.78	2940	6.16	721	2.81	129	1.85	16.8	66.68	8.52	2.49	0.278	0.994094	0.0798	0.062
148.56	95.86	3.52	8.30	4010	10.21	947	4.73	171	7.74	16.8[b]	59.27	8.05	2.09	0.278	0.992473	0.085[c]	0.039
197.93	101.38	3.52	11.51	3860	13.56	916	5.96	171	8.40	17.2	56.34	8.06	2.10	0.278	0.990860	0.085[c]	0.037
247.05	107.13	3.52	14.90	3840	16.88	915	7.04	170	11.09	16.4	51.57	7.90	2.14	0.278	0.989264	0.092[c]	0.044

[a]Units: c, mmol dm^{-3}; τ_j, ps; ρ, kg·dm^{-3}; κ, S m^{-1}

[b]Parameter fixed in the fit.

[c]Estimated from fitting the spectra
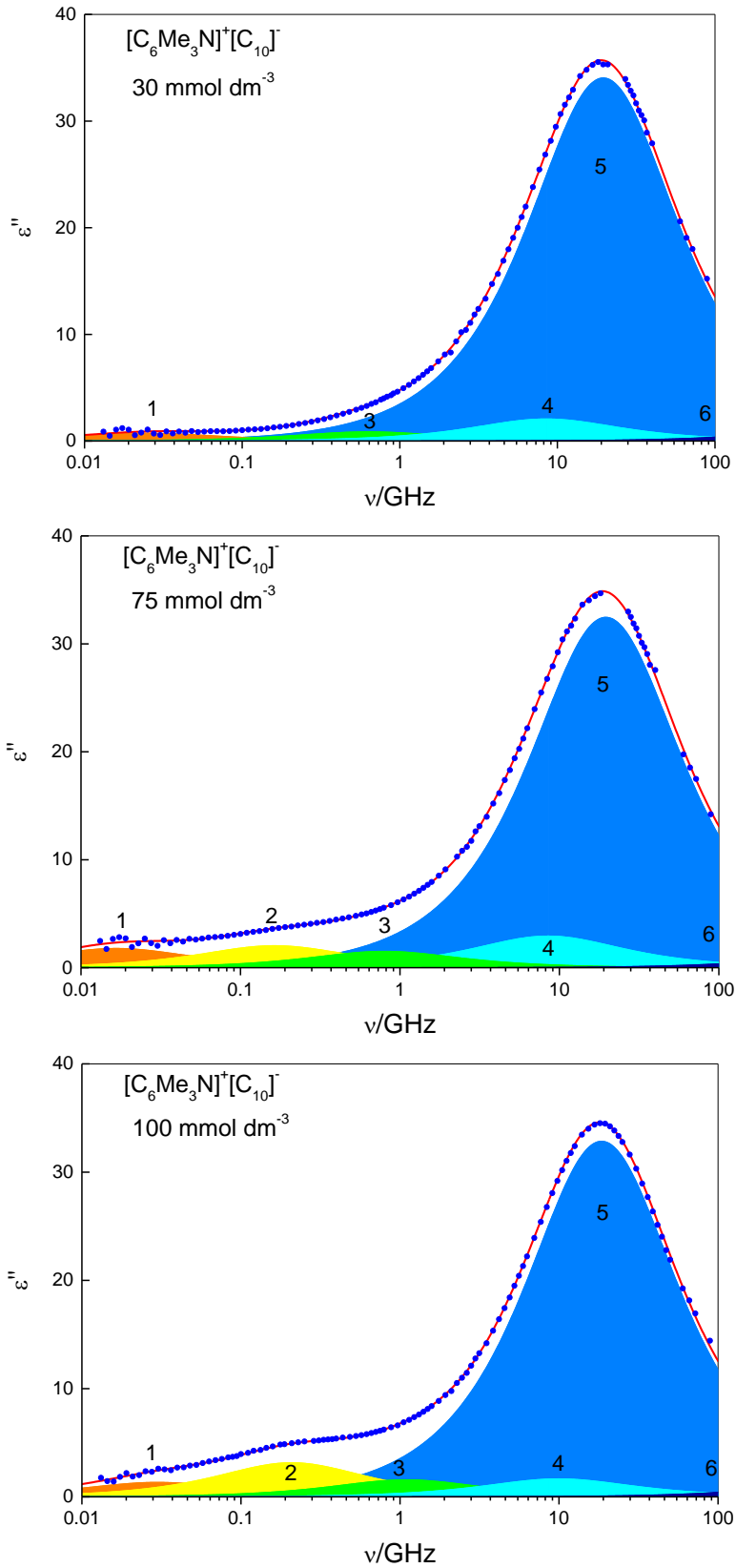
Figure S8. Dielectric loss, $\varepsilon''(\nu)$, spectrum (•) of 30, 75 and 150 mmol dm^{-3} aqueous solutions of [C$_6$Me$_3$N]$^+$[C$_{10}$]$^-$ at 298.15 K. The lines show the fit with the 6D model (5D model for 30 mmol dm^{-3} solution); the shaded areas indicate the contributions of the resolved modes $j = 1…6$.
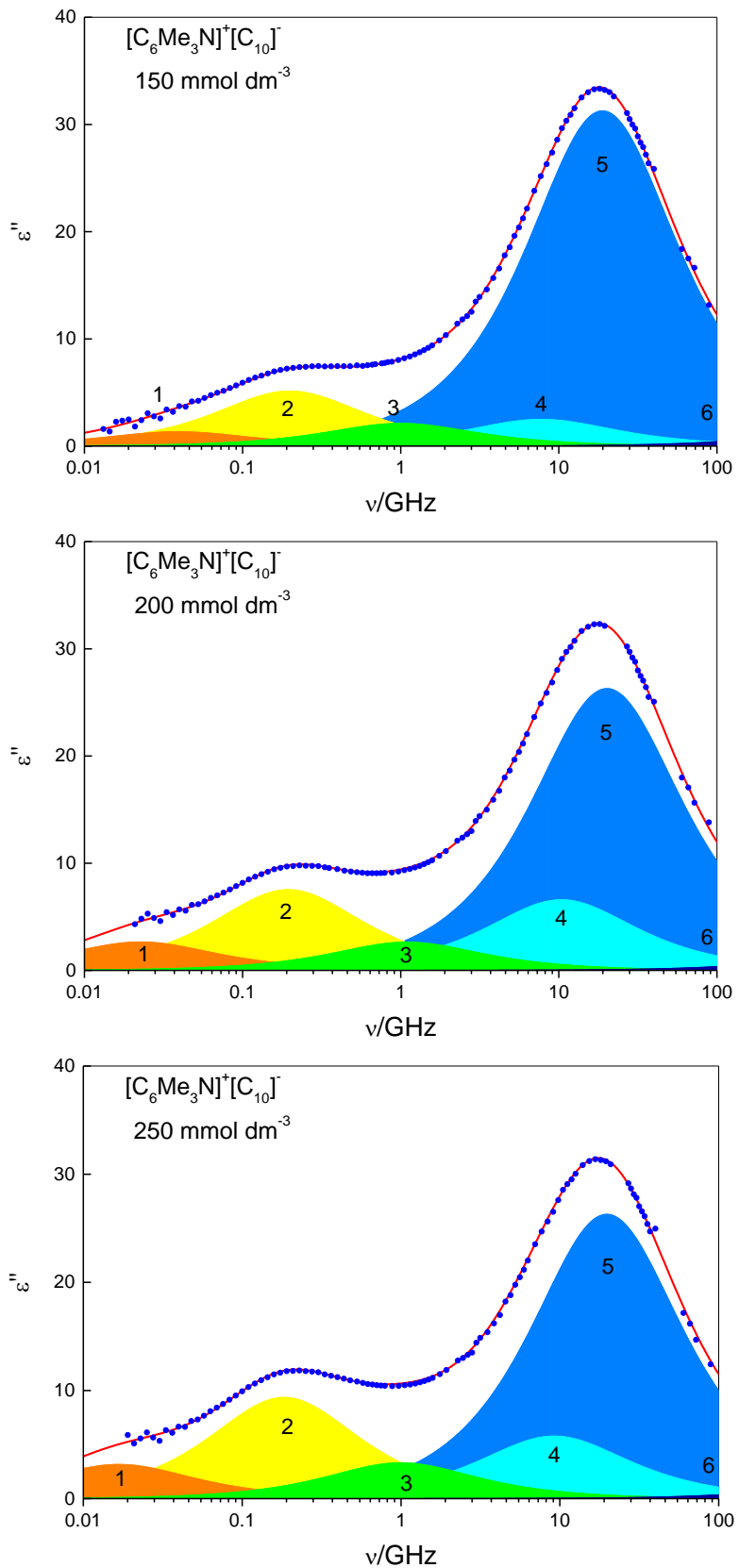
Figure S9. Dielectric loss, $\varepsilon''(\nu)$, spectrum (●) of 150, 200 and 250 mmol dm^{-3} aqueous solutions of $[C_6Me_3N]^+[C_{10}]^-$ at 298.15 K. The lines show the fit with the 6D model; the shaded areas indicate the contributions of the resolved modes $j = 1\dots6$.
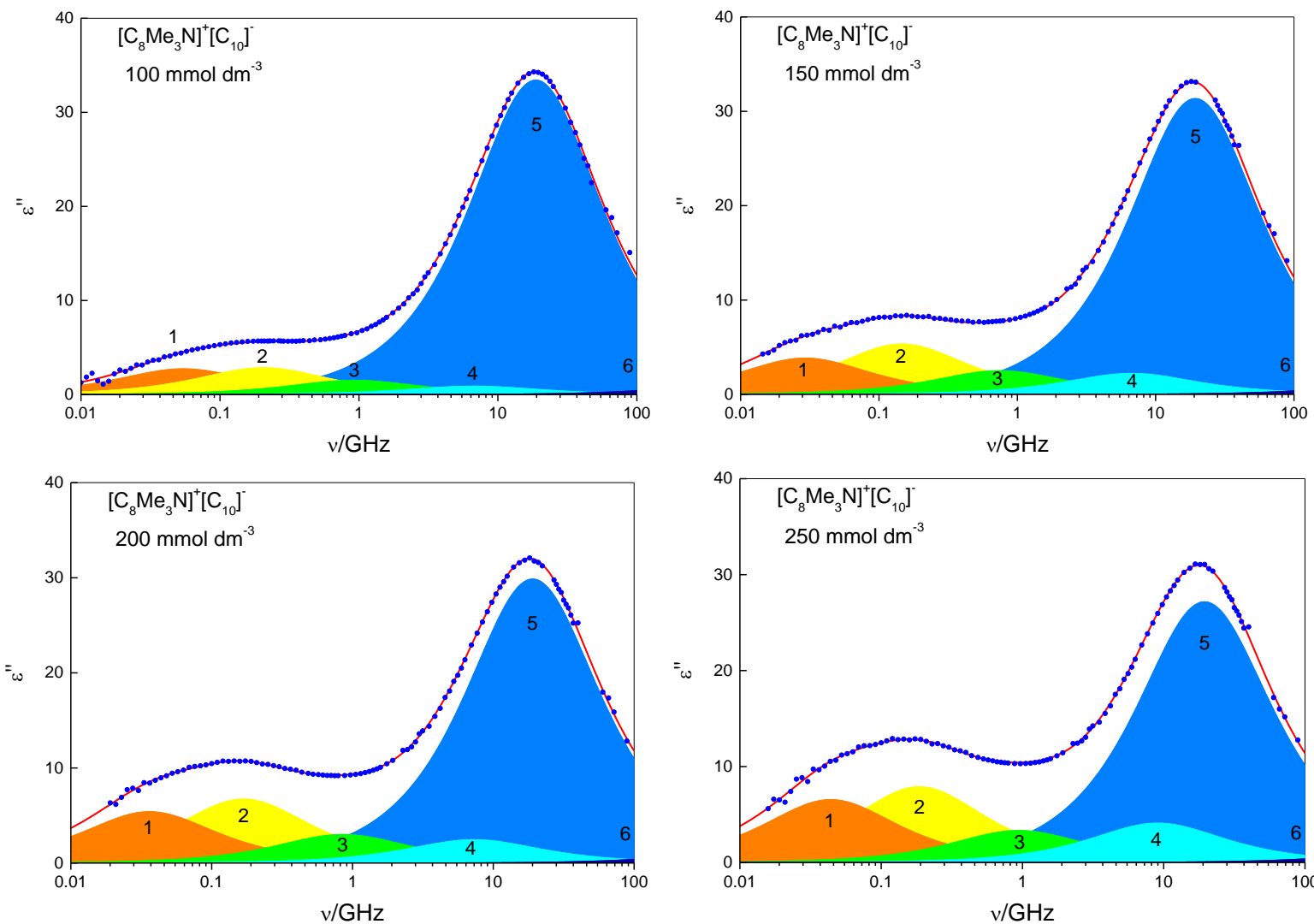
Figure S10. Dielectric loss, $\varepsilon''(\nu)$, spectrum ($\bullet$) of 100, 150, 200 and 250 mmol dm^{-3} aqueous solutions of $[C_8Me_3N]^+[C_{10}]^-$ at 298.15 K. The lines show the fit with the 6D model; the shaded areas indicate the contributions of the resolved modes $j = 1\ldots6$.
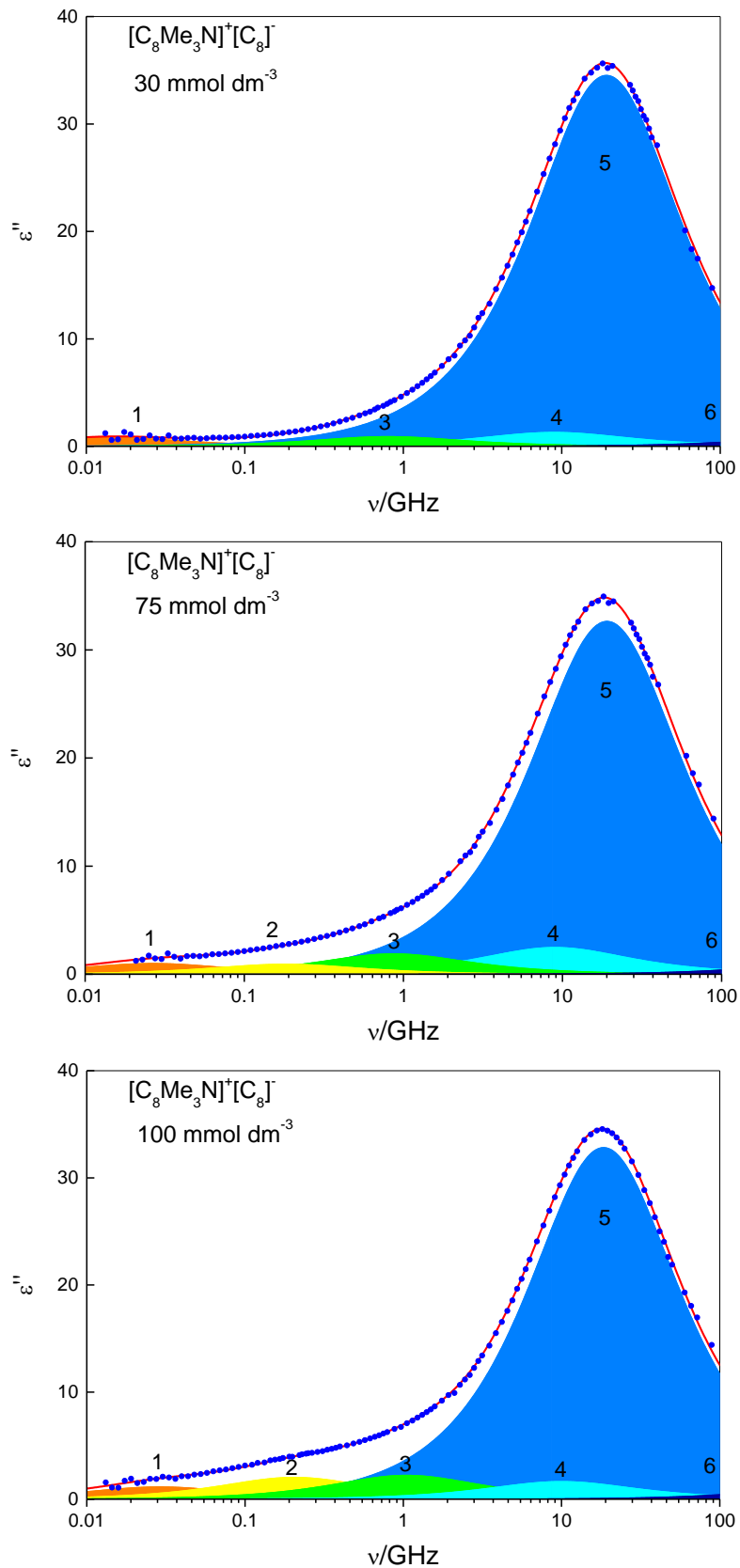
Figure S11. Dielectric loss, $\varepsilon''(\nu)$, spectrum ($\bullet$) of 30, 75 and 150 mmol dm^{-3} aqueous solutions of [C$_8$Me$_3$N]$^+$[C$_8$]$^-$ at 298.15 K. The lines show the fit with the 6D model (5D model for 30 mmol dm^{-3} solution); the shaded areas indicate the contributions of the resolved modes $j = 1\ldots6$.
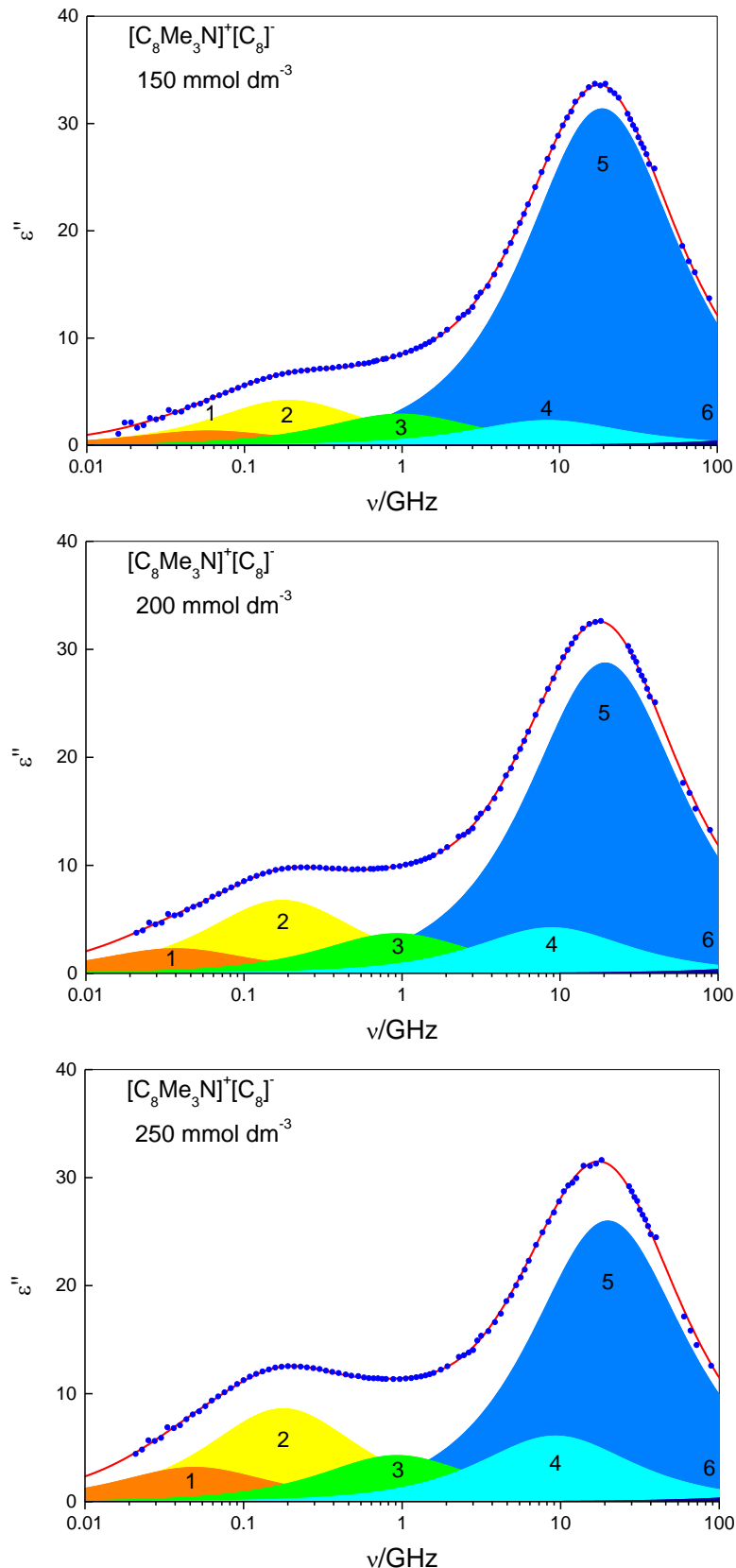
Figure S12. Dielectric loss, $\varepsilon''(\nu)$, spectrum ($\bullet$) of 150, 200 and 250 mmol dm^{-3} aqueous solutions of $[C_8Me_3N]^+[C_8]^-$ at 298.15 K. The lines show the fit with the 6D model; the shaded areas indicate the contributions of the resolved modes $j = 1\dots6$.
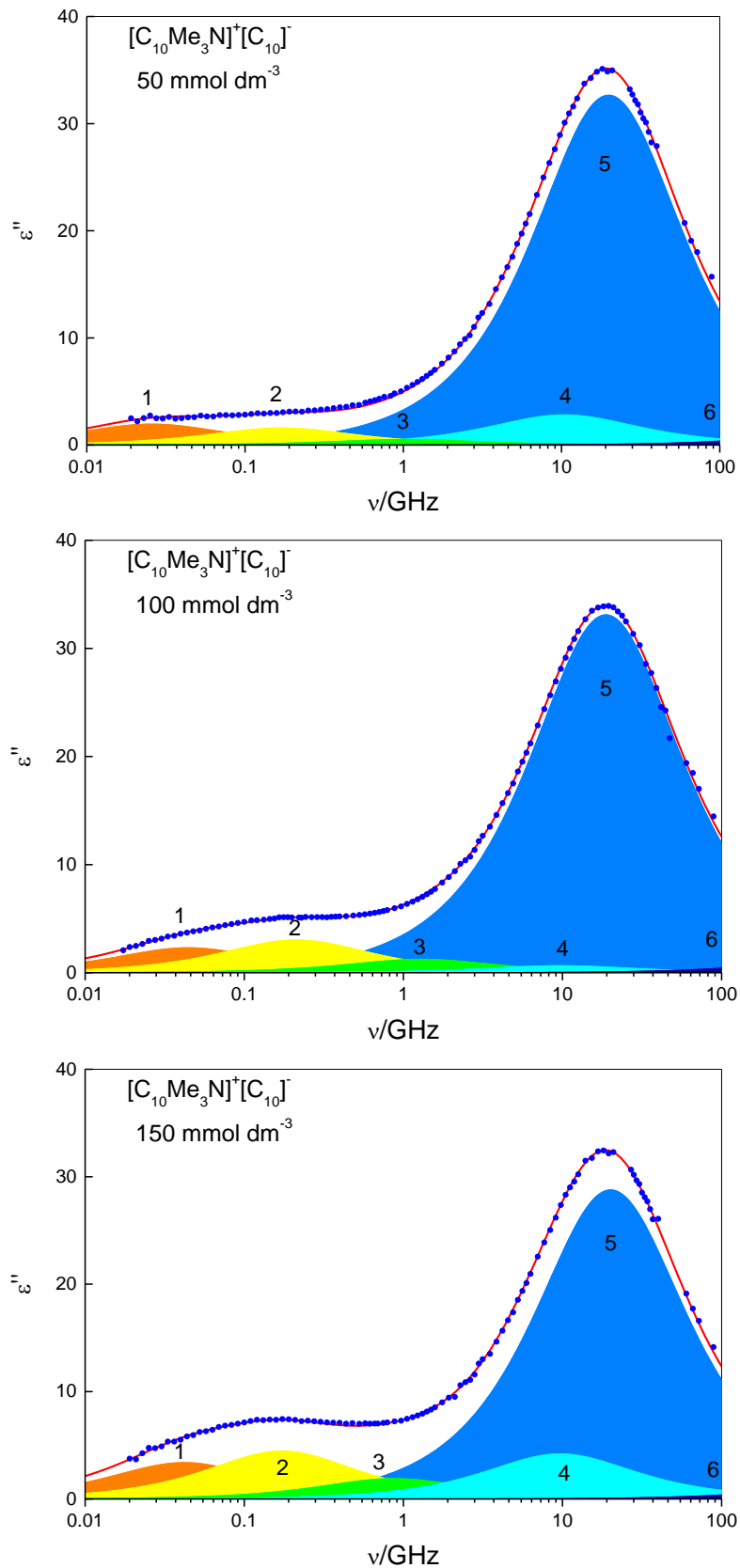
Figure S13. Dielectric loss, $\varepsilon''(\nu)$, spectrum ($\bullet$) of 50, 100 and 150 mmol dm^{-3} aqueous solutions of $[C_{10}Me_3N]^+[C_{10}]^-$ at 298.15 K. The lines show the fit with the 6D model; the shaded areas indicate the contributions of the resolved modes $j = 1\ldots6$.
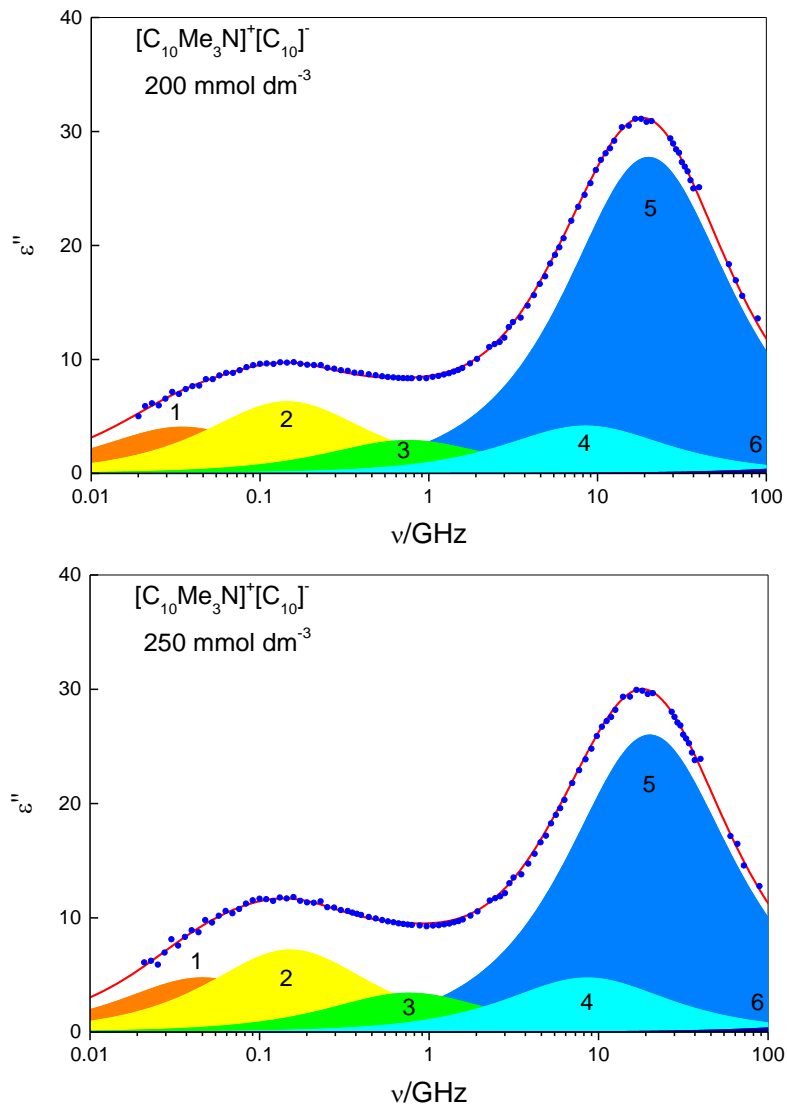
Figure S14. Dielectric loss, $\varepsilon''(\nu)$, spectrum ($\bullet$) of 200 and 250 mmol dm^{-3} aqueous solutions of $[C_{10}Me_3N]^+[C_{10}]^-$ at 298.15 K. The lines show the fit with the 6D model; the shaded areas indicate the contributions of the resolved modes $j = 1\ldots6$.
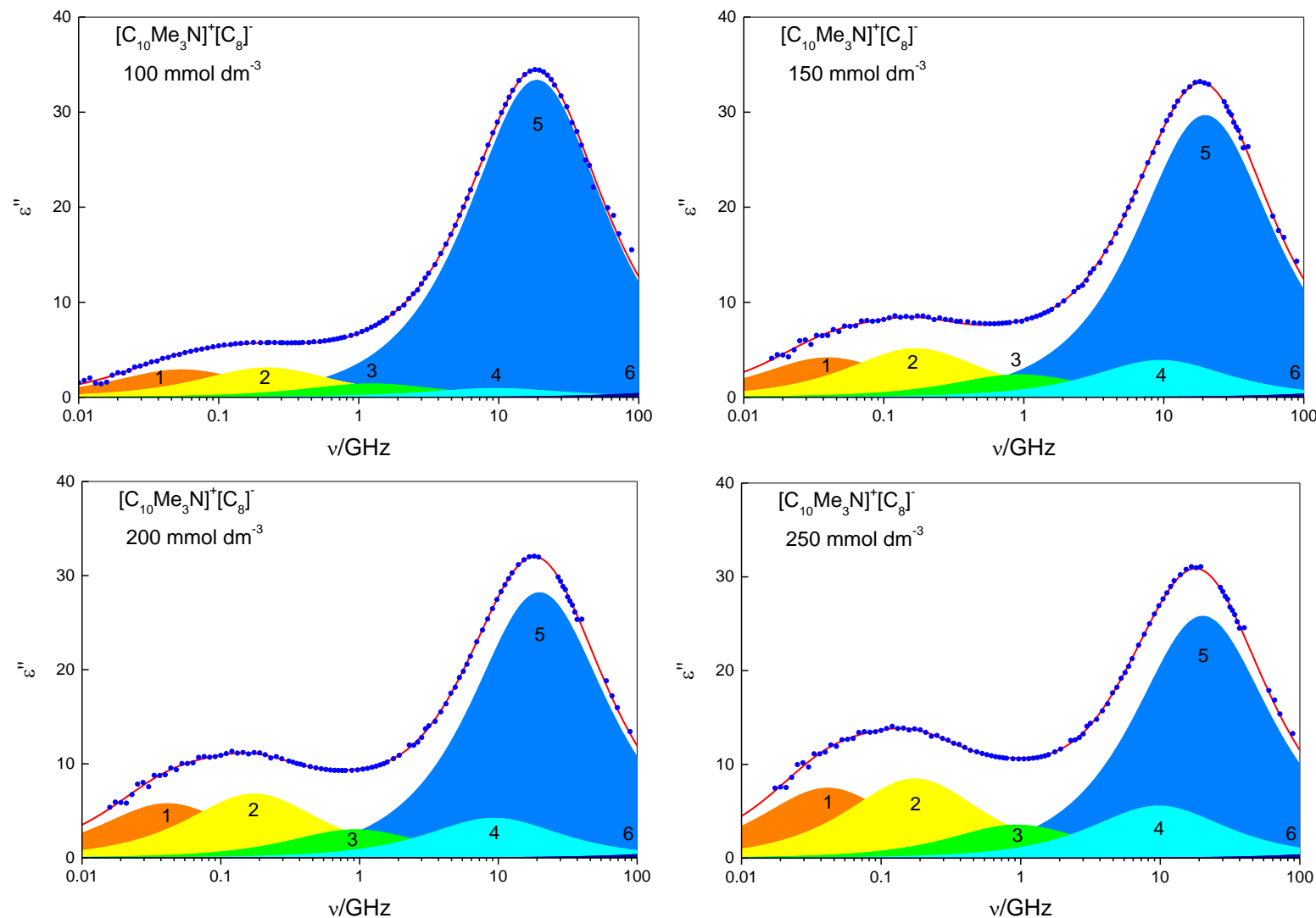
Figure S15. Dielectric loss, $\varepsilon''(\nu)$, spectrum (●) of 100, 150, 200 and 250 mmol dm^{-3} aqueous solutions of $[C_{10}Me_3N]^+[C_8]^-$ at 298.15 K. The lines show the fit with the 6D model; the shaded areas indicate the contributions of the resolved modes $j = 1\ldots6$.
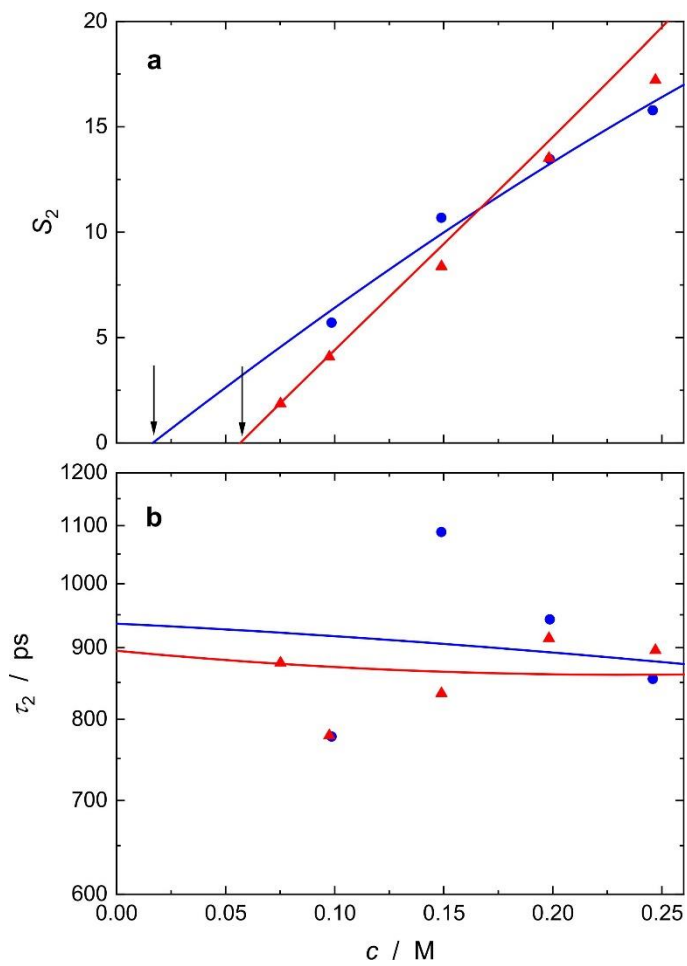
Figure S16. Solute-related amplitudes, S_2 (a) and relaxation times, τ_2 (b), of aqueous $[C_8Me_3N]^+[C_8]^-$ (red ▲) and $[C_8Me_3N]^+[C_{10}]^-$ (blue ●) and associated fits (lines) with Grosse's theory. The arrows in (a) indicate the associated *cmc* values (Table 2).
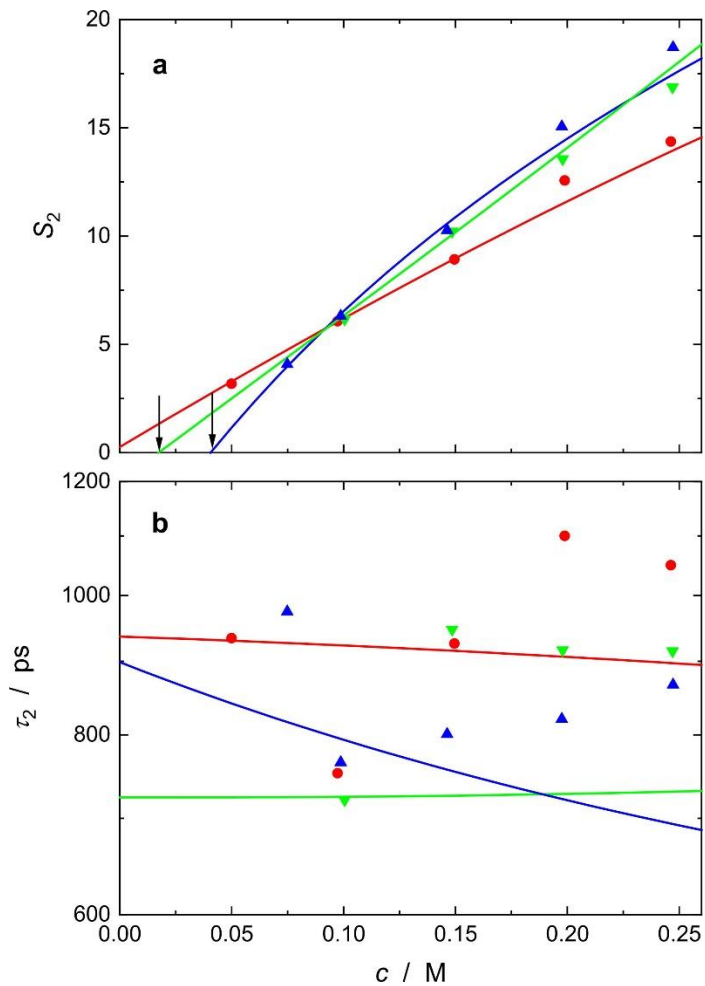
Figure S17. Solute-related amplitudes, S_2 (a) and relaxation times, τ_2 (b), of aqueous $[C_6Me_3N]^+[C_{10}]^-$ (blue ▲), $[C_{10}Me_3N]^+[C_{10}]^-$ (red ●) and $[C_{10}Me_3N]^+[C_8]^-$ (green ▼) and associated fits (lines) with Grosse's theory. The arrows in (a) indicate the associated *cmc* values (Table 2) of $[C_6Me_3N]^+[C_{10}]^-$ and $[C_{10}Me_3N]^+[C_8]^-$.

Estimation of bare and hydrated micelle volumes

Combining the results from the density measurements, ITC and DRS allows estimating the size of the micelles. From the apparent molar volume of the surfactant in the micelle, V_ϕ^M, (Table 1) and the average aggregation number, n_{avg} (Figures S6 and S7), the volume of the "bare" micelle, V_{bare}^M, can be obtained as

$$V_{bare}^M = n_{avg} V_\phi^M / 2 / N_A \qquad \text{(xxxvii)}$$

To obtain the volume of the micelle, V^M, the water molecules in-between the alkyl chains and the polar heads of the ions are added to V_{bare}^M

$$V^M = V_{bare}^M + n_{avg} Z_{s3}^M V_m(H_2O) / 2 / N_A \qquad \text{(xxxviii)}$$

where $V_m(H_2O)$ is the molar volume of water, 18.069 cm^3 mol^{-1} at 298.15 K. By taking into the account all of the water slowed down by the micelle the hydrated volume of the micelle, V_{hyd}^M, is given by

$$V_{hyd}^M = V_{bare}^M + n_{avg} Z_t^M V_m(H_2O) / 2 / N_A \qquad \text{(xxxix)}$$

Assuming spherical micelles, the radii of bare, r_{bare}^M, with inserted water molecules, r^M, and hydrated micelles, r_{hyd}^M, gathered in Table 4 were obtained. Since, the concentration dependence of the values is within the experimental uncertainty only values for 250 mmol dm^{-3} solutions are presented.

Table S7. Average aggregation number, n_{avg}, volumes of the bare micelle, V_{bare}^M, micelle, V^M, and hydrated micelle, V_{hyd}^M, and corresponding micelle radii, r_{bare}^M, r^M and r_{hyd}^M, for 250 mmol dm^{-3} aqueous solutions at 298.15 K.[a,b]

	n_{avg}	V_{bare}^M	V^M	V_{hyd}^M	r_{bare}^M	r^M	r_{hyd}^M
$[C_6Me_3N]^+[C_{10}]^-$	25	7.0	11.2	22.0	1.19	1.39	1.74
$[C_8Me_3N]^+[C_{10}]^-$	29	8.8	13.9	21.0	1.28	1.49	1.71
$[C_8Me_3N]^+[C_8]^-$	20	5.6	9.9	16.0	1.10	1.33	1.56
$[C_{10}Me_3N]^+[C_{10}]^-$	34	11.6	18.6	38.8	1.40	1.64	2.10
$[C_{10}Me_3N]^+[C_8]^-$	31	9.5	15.2	28.9	1.31	1.54	1.90

[a]Units: V_{bare}^M, V^M, V_{hyd}^M in nm^3; r_{bare}^M, r^M, r_{hyd}^M in nm;
[b]Uncertainty: n_{avg}: ±2; V^M, V_{hyd}^M: ±1; r^M, r_{hyd}^M: ±0.1.

References

(1) Herington, E.F.G. Recommended reference materials for the realization of physical properties – density. *Pure Appl. Chem.* **1976**, *45*, 1–9.

(2) Eriksson, P.-O.; Lindblom, G.; Burnell, E.E.; Tiddy, G.J.T. Influence of organic solutes on the self-diffusion of water as studied by nuclear magnetic resonance spectroscopy. *J. Chem. Soc. Faraday Trans. I* **1988**, *84*, 3129–3139.

(3) Woolley, E. M.; Burchfield, T. E. Model for thermodynamics of ionic surfactant solutions. 2. enthalpies, heat capacities, and volumes. *J. Phys. Chem.* **1984**, *88*, 2155–2163.

(4) Prabhu, N. V.; Sharp, K. Heat Capacity in Proteins. *Annu. Rev. Phys. Chem.* **2005**, *56*, 521–548.

(5) Loladze, V. V.; Ermolenko, D. N.; Makhatadze, G. I. Heat capacity changes upon burial of polar and nonpolar groups in proteins. *Protein Sci.* **2001**, *10*, 1343–1352.

(6) Spolar, R.S.; Livingstone, J.R.; Record Jr., M.T. Use of liquid hydrocarbon and amide transfer data to estimate contributions to thermodynamic functions of protein folding from the removal of nonpolar and polar surface from water. *Biochemistry* **1992**, *31*, 3947–3955.